Photopolymerization and Photostructuring of Molecularly Imprinted Polymers

Ernesto Iii Paruli, Olivier Soppera, Karsten Haupt, Carlo Gonzato

Photopolymerization and Photostructuring of Molecularly Imprinted Polymers

Ernesto III Paruli,[a] Olivier Soppera,[b,c] Karsten Haupt[a] and Carlo Gonzato*[a]*

[a] Université de Technologie de Compiègne, CNRS Laboratory for Enzyme and Cell Engineering, 60203 Compiègne, France. [b]Université de Haute-Alsace, CNRS Mulhouse Materials Science Institute, 68100 Mulhouse, France. [c]Université de Strasbourg, 67081 Strasbourg, France.

KEYWORDS. Molecularly imprinted polymers, photopolymerization, photostructuring, mask lithography, maskless lithography, stereolithography, microstructures, nanostructures

ABSTRACT. Over the past few decades, molecularly imprinted polymers (MIPs) have become extremely attractive materials for biomimetic molecular recognition, thanks to their excellent affinity and specificity, combined with robustness, easy engineering and competitive costs. MIPs are synthetic antibody mimics obtained by the synthesis of 3D polymer networks around template molecules, thus generating specific binding cavities. Numerous efforts have been made to improve the performances and the versatility of MIPs, with a special focus on ways to control their size, morphology, and physical form for a given application. Gaining control over these parameters has allowed MIPs to adopt a defined micro- and nano-structure, providing access to nanocomposites and micro-/nano-systems, with fine-tuned properties, which become critical for modern

applications ranging from chemical sensing to bioimaging and medical therapy. In this rich and complex context, light as a cheap and versatile source of energy has emerged as a powerful tool for structuring MIPs. This review presents the most recent advances on structuring MIPs at the nano-/micro-scale, using light as a *stimulus* to trigger the polymerization process. Thus, after a general introduction on radical polymerization of MIPs, with a special emphasis on photopolymerization by UV and visible light, the reader will be presented with ways of structuring MIPs by processes that are inherently spatially confined, such a localized photopolymerization and lithographic techniques, supported by representative examples and complemented with a final outlook on future trends in this field.

ABBREVIATIONS

2,4-D, 2,4-dichlorophenoxyacetic acid; 4-VP, 4-vinylpyridine; AA, acrylic acid; AAm, acrylamide; AB·HCl, N-acryloyl-p-aminobenzamidine dihydrochloride; ACN, acetonitrile; AFM, atomic force microscopy; AIBN, azobisisobutyronitrile; ATRP, atom-transfer radical polymerization; AuNP, gold nanoparticle; BAPO, bisacylphosphine oxide; BSA, bovine serum albumin; CAD, computer-aided design; CDTPA 4-cyano-4-[(dodecylsulfanylthiocarbonyl)sulfanyl]pentanoic acid; CPADB, 4-cyano-4-(thiobenzoylthio)pentanoic acid; CPDTC, 2-cyano-2-propyldodecyltrithiocarbonate; CETP, 4-cyano-4-ethyltrithiopentanoic acid; ENRO, enrofloxacin; DABP, 4,4'-bis(di-n-butylamino)biphenyl; DCM, dichloromethane; DEAEM, diethylaminoethyl methacrylate; DEDTC, diethyldithiocarbamate; DMA, N,N-dimethylaniline; DMF, N,N-dimethylformamide; DMPA, 2,2-dimethoxy-2-phenylacetophenone; DMSO, dimethylsulfoxide;

DVB, divinylbenzene; EBAAm, N,N'-ethylenebis(acrylamide); EBL, electron-beam lithography; ECL, electrochemiluminescence; EDMAT, 2-(((ethylthio)carbonothioyl)thio)-2-methylpropanoic acid; EGDMA, ethylene glycol dimethacrylate; EIS, electrochemical impedance spectroscopy; EtOH, ethanol; FIBL, focused-ion-beam lithography; FRP, free-radical polymerization; GlcA, glucuronic acid; HEMA, 2-hydroxyethyl methacrylate; HOPG, highly ordered pyrolytic graphite; IR, infrared; IUPAC, International Union of Pure and Applied Chemistry; LED, light-emitting diode; LOD, limit of detection; MAA, methacrylic acid; MAM, methacrylamide; MBAAm, N,N′-methylenebisacrylamide; MBIL, multibeam interference lithography; MEMS, microelectromechanical system; MIP, molecularly imprinted polymer; MSLA, multiphoton stereolithography; MUCP, magnetic upconverting particle; NANA, N-acetylneuraminic acid; NEMS, nanoelectromechanical system; NIL, nanoimprint lithography; NIP, non-imprinted polymer; NIR, near infrared; NMR, nuclear magnetic resonance; NOBE, N,O-bismethacryloyl ethanolamine; PDMS, polydimethylsiloxane; PEG200DMA, poly(ethyleneglycol(200))dimethacrylate; PET, photo-electron transfer; PETA, pentaerythritol triacrylate; PEW, polymerization by evanescent wave; PMMA, poly(methyl methacrylate); QD, quantum dot; RDRP, reversible deactivation radical polymerization; RAFT, reversible addition-fragmentation chain-transfer polymerization; SFRP, stable free radical polymerization; SIP, surface imprinted polymer; SLA, stereolithography; SOI, silicon-on-insulator; SPE, solid-phase extraction; STEM, stimulated-emission-depletion microscopy; TEA, triethylamine; TED, tetraethylthiuram disulfide; TEM, transmission electron microscopy; TPO, (2,4,6-trimethylbenzoyl)phosphine oxide; TPO-L, ethyl (2,4,6-trimethylbenzoyl) phenylphosphinate; TPS, two-photon stereolithography; UV, ultraviolet; V-50, 2,2'-azobis(2- methylpropionamidine)

dihydrochloride; VIS, visible; Z-L-Phe, carbobenzyloxy-L-phenylalanine; μCP microcontact printing; μFP, microfluidic printing; μSL, microstereolithography.

I. Introduction - Molecularly imprinted polymers

Molecular recognition is an underlying phenomenon of many biochemical processes, which has also a number of important practical applications. In Nature, antibodies and enzymes are known to bear binding sites that recognize their respective antigens and substrates with high affinity and selectivity, thus ensuring their physiological functions.[1–4] These "high-precision" host-guest interactions have inspired the design of many synthetic recognition systems (e.g. aptamers, metal organic frameworks, dendrimers, crown ethers), including molecularly imprinted polymers (MIPs), which are considered one of the simplest though elegant ways to generate synthetic molecular recognition systems. MIPs have been dubbed "plastic antibodies" as they mimic in artificial polymeric matrices the recognition phenomena occurring in natural biomolecules, thus they are an excellent example of biomimicry at the molecular level. Although the first evidence of imprinting was serendipity reported in the early '30s by Polyakov while attempting to modify silica for chromatographic purposes,[5] the "modern era" of molecular imprinting was launched with the seminal works of Wulff[6] and Mosbach[7] in the '70s and '80s.

MIPs are synthetic polymers displaying high affinity and selectivity for analytes ranging from ions,[8–10] to small organic molecules,[11–13] peptides,[14–16] biomolecules[17–19], up to viruses[20–22] and whole cells.[23,24] In the majority of the reports, a template polymerization approach is used, that is, a polymer is synthesized in the presence of a molecular template, which results in the generation of specific 'cavities'. There are a few examples, though, where MIPs have been obtained from pre-formed polymers which are molded around the template.[25,26] In the template polymerization

approach, the crucial step in the preparation of a MIP involves the formation of a pre-polymerization complex based on non-covalent interactions[27,28] (or in some cases, reversible covalent bonds[6]) between functional monomers and a target molecule, or a derivative thereof, which serves as the template (Figure 1). This pre-polymerization complex is then polymerized with an excess of cross-linker in order to "freeze" its structure into a three-dimensional rigid matrix. Thus, after polymerization and template removal, cavities are created in the polymer network that are complementary to the template in terms of size, shape and spatial distribution of functional groups. As such, the polymer is effectively "imprinted" and its binding sites locally display a "ligands sphere" able to host the template with affinities comparable to those of antibodies. At the same time, MIPs surpass their natural counterparts in terms of physical stability, physico-chemical and biochemical resistance, robustness and low-cost due to their synthetic polymeric nature. Thanks to these advantages, MIPs have been exploited in diverse applications requiring molecular recognition such as affinity separation,[29–32] drug delivery,[33–35] drugs,[36] bioimaging,[37–39] cosmetics,[40] catalysis[41–43] and chemical sensing.[44–47]

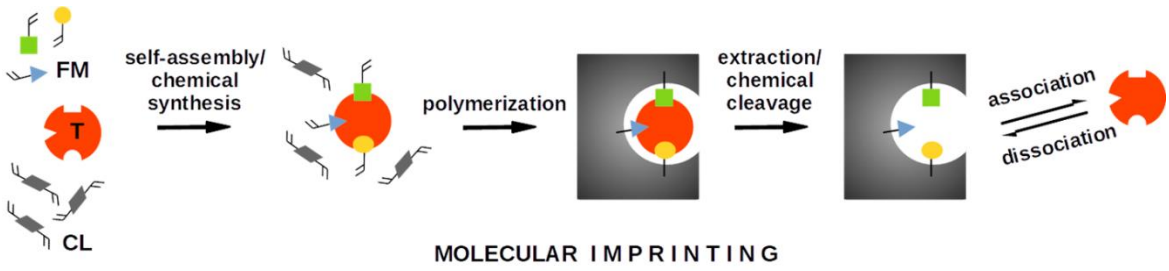

Figure 1. General scheme for the molecular imprinting of polymers: Functional monomers (FM) self-assemble around a template (T) to form a pre-polymerization complex which undergoes polymerization in the presence of a cross-linker (CL). Upon template extraction, binding sites become available for the template uptake.

An important aspect to consider when synthesizing a MIP is the way of triggering its polymerization, as this choice affects the reaction conditions and thus the resulting MIP properties. Except for silica-based MIPs made by sol-gel chemistry (i.e. obtained by hydrolysis-polycondensation), imprinted polymers are usually synthesized by electrochemically, thermally, photochemically or redox-initiated chain-reaction. Electropolymerization of electroactive monomers such as pyrrole, aniline or dopamine is a technique based on a redox process or a potential sweep[48] which is especially suited for depositing polymer films directly on electrodes for electrochemical sensors, since it allows controlling the rate of polymer growth, film thickness and film morphology. Unfortunately, this technique is limited to a restricted number of functional monomers, which in turn limits the functionalities available for molecular imprinting. Redox-initiated radical polymerization is also used for MIPs synthesis, and thanks to its ability to generate radicals under mild conditions, it is especially suited for the imprinting of proteins[49] or peptides[50] in aqueous *media*.

Conversely to electrochemical and redox polymerization, thermal polymerizations use thermal initiators to generate radicals and initiate the polymerization. Mostly based on azobis- or peroxy-derivatives,[51,52] such initiators cover a large range of temperatures thanks to the possibility of modulating their half-lives at a given temperature with changes in their chemical structure. Thermal polymerization accounts for a great majority of (meth)acrylic and styrenic MIPs, with reaction temperatures usually spanning from room temperature to roughly 60°C.

Photopolymerization is another very common technique for MIPs, wherein radicals are generated upon photo-induced or photo-promoted dissociation of suitable initiating species. This approach has over the recent years gained much importance and is today often the method of choice. *So why photopolymerization?* There are two main reasons: *Firstly*, since light is directly

responsible for radical generation, the temperature can be set to low values, which protects temperature-sensitive, non-covalent interactions between template and functional monomers, thus improving the imprinting efficiency and the MIP's affinity for its target.[53] Also, the use of low temperatures (e.g. 0°C to 20°C)[54,55] is preferred to avoid degradation of sensitive analytes such as proteins[56] and in some cases, to suppress undesired side reactions.[57]

Secondly, owing to their nature, photochemical processes allow spatiotemporal and intensity control over the polymerization reaction. By simply turning on or off the light source, the radical generation can instantaneously be "switched on" or "off" in a much more efficient way compared to the other approaches such as thermal polymerization. This is especially useful in photo-induced controlled radical polymerizations, officially referred to as reversible-deactivation radical polymerizations (RDRP), wherein the molecular weight of growing polymers directly relates to monomer conversion[58] and can thus be controlled by the irradiation time. RDRPs are well-established in the imprinting field thanks to their ability to easily chain-extend with consecutive blocks and to inherently boost the binding properties of MIPs compared to free radical polymerization (FRP). The reader who is interested in this topic is invited to refer to the following representative review and research articles.[27,59–61]

Light can also be confined into limited volumes to arbitrarily initiate localized polymerizations in restricted regions, as seen in various photolithographic and 3D printing techniques (i.e. spatial control). Adjusting the wavelength and the intensity of light sources allows the manipulation of the polymerization rate *via* controlling the number of generated radicals, similarly to variating the temperature in a thermal polymerization.[58,62] All these features, which also include relatively low costs and availability of a range of light sources (i.e. lamps, LED, lasers, UV plasma sources,

sunlight),[62,63] make photopolymerization a convenient strategy for precise, hierarchical structuring and even automation in the design and fabrication of MIPs.

II. Photopolymerization of MIPs

II.1. Introduction to photopolymerization

Photoinitiation is a process wherein a light-sensitive system (called a photoinitiator) achieves, upon absorption of a suitable photon, an excited state that leads to a reactive species capable of initiating the polymerization of monomers (i.e. photopolymerization).[64,65] Depending on the nature of the photogenerated reactive species and on the chosen monomers, the polymerization can follow radical, cationic or anionic acid/base growing mechanism. If this variety provides the user with a wide choice of experimental setups, the reader should be aware that not all previously mentioned techniques are suited to the synthesis of MIPs. Indeed, in order to promote a strong interaction between the template and the functional monomers, the photoinitiating system should not interfere with them. If this can normally be achieved by formulating the photoinitiator in low molar amounts, this requirement can also be met by selecting initiating species that show poor reactivity toward common chemical functionalities in both their fundamental and excited state. Among the cited polymerization pathways (i.e. radical, cationic or anionic), the radical mechanism exhibits the best compatibility with the chemical functionalities borne by the different components of a MIP pre-polymerization mixture, which can be rather complex. Thus, over the years, radical polymerization has become the most viable solution for MIPs, due to its tolerance for many common functional groups as well as to the commercial availability of a wide range of (meth)acrylic and styrenic monomers.[66,67]

II.2. Radical photoinitiators

From the physico-chemical point of view, free radical photoinitiators are divided into two main categories: Type I and Type II photoinitiators. Type I photoinitiators undergo unimolecular homolytic bond cleavage upon excitation, to generate radicals (Figure 2A). They vary considerably in structure but prominent examples are aromatic carbonyl compounds such as acetophenone derivatives, benzoin derivatives, benzylketals, hydroxyalkylphenones and acyl (TPO) and diacyl (BAPO) phosphines.[51,68] Azoinitiators, notably AIBN, can also act as photoinitiators beyond being thermal initiators. From a general standpoint, ideal Type I photoinitiators should: (1) feature a high extinction coefficient at the selected (irradiation) wavelength to efficiently generate excited states (singlets), (2) provide a high internal conversion from singlets to (dissociative) triplet states, which in turn afford radicals by bond scission and (3) generate highly reactive radicals capable of triggering the polymerization of monomers.[52,64,69]

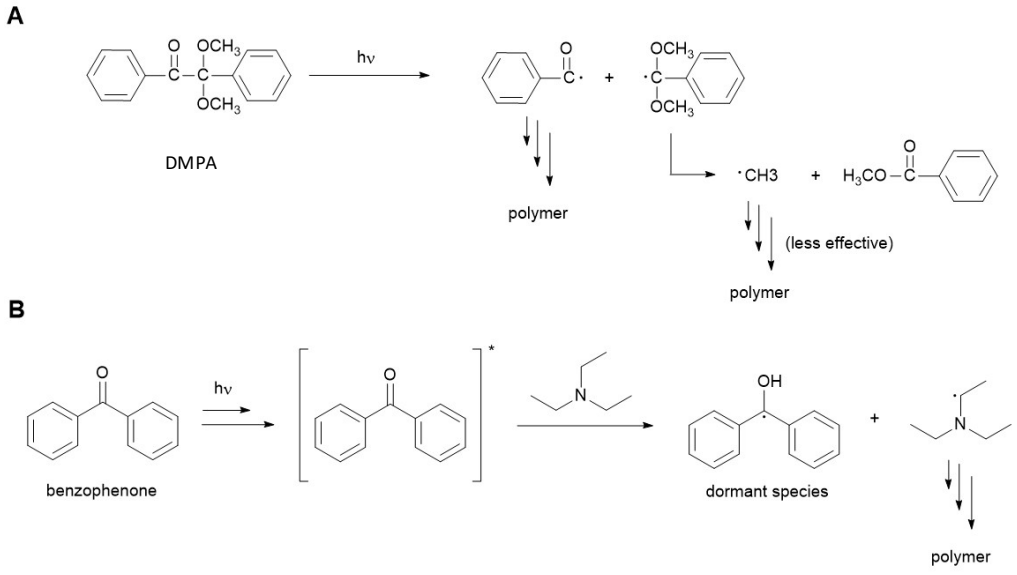

Figure 2. The initiating mechanism of a representative (A) Type I photoinitiator (dimethoxy-2-phenylacetophenone, DMPA) and (B) Type II photoinitiator. Figure 2B reproduced with permission from ref 70, copyright 2014 Wiley-VCH Verlag GmbH & Co. KGaA.

Type II photoinitiators on the other hand, do not undergo bond cleavage; instead, they get excited to a triplet state and proceed to hydrogen abstraction from a donor (also known as a co-initiator, usually an alcohol or amine) thus generating an initiating radical (Figure 2B). Since this process involves a bimolecular reaction, Type II activation occurs more slowly than Type I activation and their efficiency is diffusion-controlled. Camphorquinones, benzophenones, thioxanthones and many visible-light-activated initiators are representative examples of this second category.[52,71,72] One of the advantages of these systems is to allow extending the wavelength range by the choice of the suitable photosensitizer from the high UV up to the near infrared (NIR) (300 nm - 1064 nm).[73–76] On the other hand, the need for one, or more, coinitiators makes Type II photoinitiating systems less suitable than Type I for MIPs. Indeed, the increased number of chemicals required for a Type II photoinitiation, may interfere with the self-assembly process between template and functional monomer(s). A list of Type I and Type II photoinitiators widely used for radical polymerization, together with their excitation wavelengths, has recently been published by Lalevée and coworkers.[63]

II.3. Photo-induced controlled/living radical polymerization

FRP has proven over the years to be an extremely versatile and convenient way of synthesizing polymers in general, and also MIPs. However, it suffers from some limitations. For instance, it does not allow controlling the length of polymer chains, the size of polymer nanospheres, or the thickness of polymer layers in composite materials. Also, fine-tuning the surface properties of, and attachment of special functional groups to polymer materials through extension with polymer blocks is difficult. These limitations are inherently related to the reaction mechanism of FRP, wherein 'dead' polymer chains are created by irreversible termination, and where the strong

competition between chain growth, irreversible termination and chain transfer, does not allow to control the molecular weight of polymers.

These limitations have been overcome thanks to the development of reversible-deactivation radical polymerizations (RDRPs), previously referred to as 'controlled/living radical polymerizations', which introduced reversible dormant forms for propagating species. Having a high number of such species and only a low number of active radicals, which can quickly and reversibly switch into dormant species, is of capital importance in order to decrease the probability of irreversible termination and uncontrolled chain-transfer.[77] This has been achieved mainly by two different approaches, namely (1) reversible termination and (2) reversible transfer.

RDRPs thus allow controlling the molecular weight of growing species *via* the extent of monomer conversion, while simultaneously ensuring low polydispersity on polymer chains (i.e. < 1.3). Various techniques are currently available to perform RDRPs, which will not be detailed here. The reader is invited to refer to the following representative reviews for a wider introduction and deeper discussion on different RDRPs.[58,78,79] In the case of MIPs, the most frequently applied RDRPs are ATRP, RAFT and Iniferter polymerizations.[27]

Atom Transfer Radical Polymerisation (ATRP) (Figure 3A), which belongs to the family of 'reversible termination', relies on alkyl-halide initiators that are reversibly activated into propagating radicals via a catalyst-mediated redox process (usually a ligated metal complex[80–82] or an organo catalyst).[83,84]

A chain-transfer mechanism operating faster than chain propagation is at the basis of Reversible Addition-Fragmentation chain-Transfer radical polymerization (RAFT) (Figure 3B), wherein dithioesters and trithiocarbonates are used as chain transfer agents ('RAFT agents').[85–88] Conversely to iniferter polymerization (see below), RAFT polymerization requires both a RAFT

agent and an exogenous source of radicals (conventional radical initiator) and does not control the termination step.

Iniferters (the term stands for *ini*tiator, trans*fer* agent and *ter*minator) (Figure 3C) are situated between these two approaches since they operate through reversible termination and reversible transfer.[89] They can control a polymerization in either a photo- or heat-driven context. Introduced in the early '80s, iniferter polymerization usually involves dithiocarbamates which, irradiated with near-visible UV light,[90–93] simultaneously behave as initiator, transfer agent and terminator. Recently, trithiocarbonates have also been included among (photo)iniferters, since their dissociation can be triggered with visible light.[94,95] Other examples are thiocarbonylthio, thiuram disulfides, peroxides, tetraphenylethanes, sulfides, phenylazo compounds, amines, alkoxyamines and halides.[89]

Overall, the use of RDRPs for the synthesis of polymers and also MIPs has allowed controlling feature size such as the thickness of the polymer layers or the particle diameter, and also tuning their surface-chemistry. In some cases, controlled polymerization also allowed to increase the affinity of the MIP for its target compared to MIPs synthesized by FRP, by favoring a more regular network structure.[27]

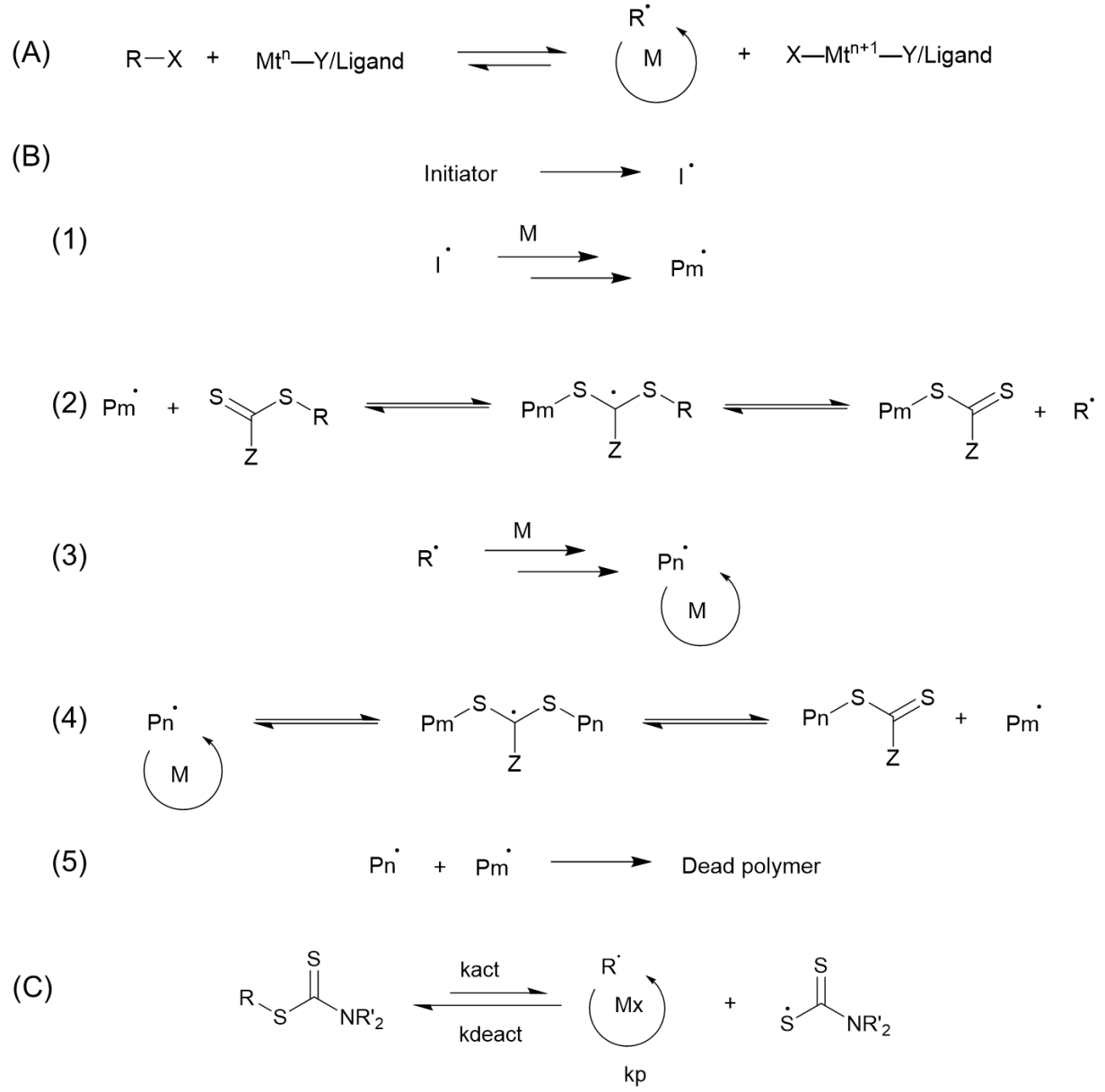

Figure 3. Mechanisms of various kinds of RDRP: (A) ATRP, (B) RAFT, and (C) iniferter polymerization. (B) RAFT polymerization proceeds by the following steps: (1) initiation, (2) RAFT pre-equilibrium, (3) propagation, (4) RAFT main equilibrium, and (5) termination.

II.4. The photopolymerization wavelength

While UV light remains a mainstay because many organic species generate radicals upon UV absorption, it also requires caution as absorption by the template and/or functional monomers may result in template degradation and/or monomer self-initiation.[95,96] For this reason, visible light has recently risen as an interesting alternative: applying initiators that specifically absorb in the visible spectrum allows to preserve sensitive molecules in solution by specifically triggering a single chemical species. This applies to conventional as well as to controlled radical polymerization, with the latter recently drawing great attention due to the possibility of easily tuning the polymer's features as detailed for instance by Johnson and co-workers.[58]

Various kinds of initiators exist for visible light photopolymerization such as some organic dyes and many organometallic compounds. Some initiators such as anthraquinone derivatives are actually Type II UV photoinitiators modified with auxochromes and extended π-π bond conjugation to shift their absorption range from the UV to the visible region.[73]

The recent use of trithiocarbonates,[97] benzyl tellurides[98] and diselenide compounds[99] as visible-active photoiniferters has considerably expanded the use of higher wavelengths for controlled/living polymerizations as well.[27,58,59,93] Also, the use of catalysts allowing for photo-electron transfer (PET) processes, as reported for instance by Hawker and co-workers,[100–102] and Boyer and co-workers,[103–107] has helped the application of longer wavelengths in photo-induced controlled radical polymerizations. During PET, light absorption causes a photo-redox catalyst to enter an excited state, which allows oxidizing or reducing a photoinitiator that in turn forms a radical able to start the polymerization.[108,109] The first successful attempt to control polymerization by means of activation/deactivation cycles mediated by blue light was reported by Fors and Hawker who used *fac*-[Ir(ppy)$_3$] as a catalyst for the atom transfer radical polymerization (ATRP)

of methyl methacrylate (MMA), with ethyl-a-bromophenylacetate as an initiator.[100] Subsequently, Boyer and his team used *fac*-[Ir(ppy)$_3$] as PET catalyst to thiocarbonyl compounds and thus to reversible addition-fragmentation chain-transfer (RAFT) polymerization.[103,107] Different kinds of catalysts have so far been applied to PET-RAFT polymerization, which have progressively allowed moving from blue to green[110] and red light (e.g. zinc porphyrins[104]) and up to the near-infrared (NIR) light thanks to the use of some pigments such as bacteriochlorophylls.[105]

NIR is particularly interesting for *in vivo* applications, as it is known to deeply penetrate biological tissues[111,112] thanks to the so called "biological window",[113] which preserves cells from photodamage and holds great promise for *in vivo* polymerizations.[71] NIR photopolymers have been initially developed for graphic industry[114] and holography.[115] The recent interest for NIR photopolymer systems is due to the potential applications in the field of in-depth photocuring.[116,117] Indeed, as light penetration is higher in the NIR region than in the UV, NIR appears as a good solution to improve the penetration depth and polymerization of thick objects and composites. Other examples of photopolymerization and photostructuration using NIR lights have also been proposed.[118–120] Typical photoinitiator systems contain an NIR dye and a co-initiator. Carbocyanines (Indocyanine Green) associated to amines have shown their efficiency for polymerization in the 780-850 nm range. Indeed, due to its low energy content, NIR cannot excite a Type I photoinitiator upon a single absorption, conversely to UV or visible light.[121]

NIR can also trigger photopolymerization through two-photon absorption, where the simultaneous absorption of two photons allows matching the energy associated with a single UV or visible photon. This phenomenon, similar to photon "upconversion" in the field of fluorescence, thus allows triggering conventional UV or visible photoinitiators *via* NIR excitation. From the chemical point of view, multiple photon absorption can occur directly on suitable photoinitiators,

such as Type I Lucirin TPO[122] and Type II 7-diethylamino-3-thenoylcoumarin,[123] or be mediated by exogenous species absorbing multiple NIR photons and returning this energy as UV or visible radiation, like upconverting phosphors.[70] A compelling example of photopolymerization mediated by NIR light was reported by Torgensen et al. who photopolymerized *via* two-photon polymerization a hydrogel which partially trapped the roundworm *Caenorhabditis elegans* as a model living organism.[124] *C. elegans* kept moving during the photopolymerization, while a short segment of its body was progressively immobilized into the growing hydrogel. This remarkable result proved that it was possible to drive a photopolymerization with NIR light in the presence of and through a living sample. The application of two-photon polymerization to the synthesis and structuring of MIPs will be discussed later in this review.

An interesting route for visible-light driven photopolymerization consists in using the emission of fluorescent nanoparticles upon excitation with shorter or longer wavelengths. For example, quantum dots (QDs) are fluorescent semiconductor nanocrystals able to emit visible light of a certain wavelength (depending on the size of the QDs) upon excitation by UV light.[125–127] Polymerization can thus be initiated by the emitted fluorescence light by using a suitable initiator that is activated by visible but not by UV light.[128] On the other hand, visible light-driven photopolymerization can also be achieved upon upconversion. Upconverting phosphors (UCPs) are lanthanide- or actinide-based nanoparticles capable of converting low-energy radiation (such as infrared) into high-energy radiation (such as visible light) through absorption of multiple photons or through energy transfer.[129,130] Again, a suitable initiator activated by visible light is needed to start the polymerization.[70]

II.5. Photopolymerization of MIPs

As previously mentioned, photopolymerization is an attractive technique for the synthesis of MIPs. Table 1 shows a selection of examples of photopolymerized MIPs with their monomers, initiators, and polymerization conditions, and imprinting template. Despite an increasing interest over the recent years in exploring different controlled photopolymerization mechanisms as outlined in the next section, free-radical polymerization (FRP) continues to be the most widely used polymerization approach to MIPs.[66] Its regular setup includes a light source, a photoinitiator and a solution of template and monomers. Light sources can be lamps, LEDs or lasers that emit at specific wavelengths in the UV or the visible range depending on the activation wavelength of the initiator.

Table 1. Non-exhaustive list of recent examples (from 2013 to 2018) of MIPs synthesized via photopolymerization.

Mechanism of Polymerization	Initiator	Initiator type	Light Source (nm)	Monomer Composition	Template	Solvent	Use	Ref
RDRP: SFRP	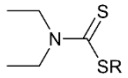 Grafted DEDTC (iniferter)	I	UV (365)	DEAEM, MBAAm	BSA	Ultrapure water	Surface film	[131]
FRP	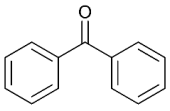 Benzophenone (TEA as hydrogen donor)	II	NIR (980) upconverted to VIS (405)	MAA, EGDMA	Enrofloxacin	DCM	Core-shell nanoparticles	[132]

Mechanism of Polymerization	Initiator	Initiator type	Light Source (nm)	Monomer Composition	Template	Solvent	Use	Ref
RDRP: RAFT	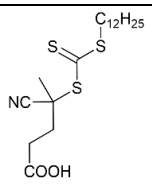 CDTPA (iniferter)	I	VIS (435 or 525)	MAA, EGDMA	Testosterone	Acetonitrile	Microspheres	[95]
RDRP: ATRP	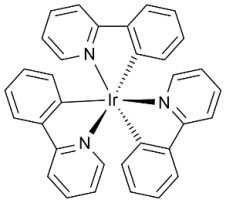 *fac*-[Ir(ppy)3] (catalyst excited by UV to reduce the initiator ethyl α -bromophenylacetate)	II	UV (365)	MAA, EGDMA	(a) Testosterone, (b) S-propranolol	(a) Toluene, (b) acetonitrile	Monoliths, films, nanoparticles	[81]
FRP	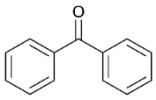 Benzophenone (grafted DMA as hydrogen donor)	II	UV (365)	MMA, EGDMA	Melamine	DMSO	Surface film	[133]
FRP	(Self-initiating monomers)	-	UV (312)	(a) AB, HEMA, EBAAm, (b) MAA or 4-VP, EGDMA or DVB	(a) Trypsin, (b) S-propranolol, 2,4-D, testosterone	(a) Sodium phosphate buffer, (b) acetonitrile or MeOH/ water	(a) Suspension, (b) bulk	[134]
FRP	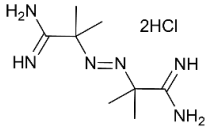 V-50	I	UV (365) via fluorescence microscope	Cyclodextrins, AAm, MBAA	Bisphenol-A	Deionized water	Microhydrogels for microvalves	[135]
FRP	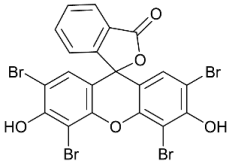 Eosin Y (TEA as hydrogen donor)	II	NIR (980) upconverted to VIS (530)	HEMA, EbAAm, AB·HCl	Trypsin	DMSO/ toluene	Core-shell NP	[70]

Mechanism of Polymerization	Initiator	Initiator type	Light Source (nm)	Monomer Composition	Template	Solvent	Use	Ref
FRP	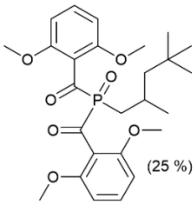 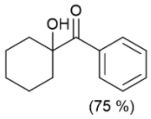 Irgacure 1800	I	UV (<400)	MAA, EGDMA	Atrazine	DCM	SPE sorbent	[136]
RDRP	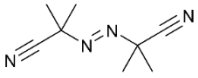 AIBN, TED as chain transfer agent	I	UV (~320-400)	DEAEM, HEMA, PEG200DMA	Diclofenac sodium	-	Gel	[66]
FRP	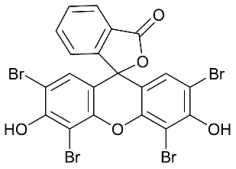 Eosin Y (MDEA as hydrogen donor)	II	VIS (532)	MAA	Rhodamine 123	ACN/DMSO	Sub-micron patterns	[96]
FRP	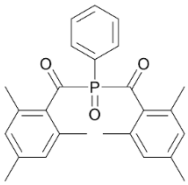 Bis(2,4,6-trimethylbenzoyl)phenyl phosphine oxide	I	UV (375)	MAA, 4-VP, EGDMA, PETA	Z-L-Phe	Tetraglyme	Microstructure	[137]
FRP	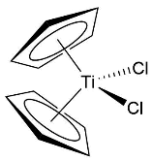 Bis(cyclopentadienyl)titanium dichloride	I	VIS (532 nm)	MAA, PETA	Testosterone	Triglyme	Hologram film	[138]

II.5.1. UV mediated photopolymerization of MIPs

The majority of photopolymerized MIPs have been prepared by conventional UV-A photopolymerization (i.e. wavelength around 365 nm), as many photoinitiators are active in this region, while monomers such as acrylates absorb weakly and are therefore relatively stable.[139]

The recent years have seen the use of UV photopolymerization for the ingenious fabrication of MIPs that transcended microspheres and monoliths. For example, Shiraki and co-workers photopolymerized cylindrical MIP microhydrogels into microchannels by projecting 365-nm UV light through a fluorescence microscope into an aqueous solution of cyclodextrin and N,N′-methylenebisacrylamide (MBAAm) monomers with the initiator 2,2'-azobis(2-methylpropionamidine) (V-50). Upon recognizing its target bisphenol-A (BPA), the MIP microhydrogel contracted and served as a self-regulating microvalve to allow automatic flow control as a function of the concentration of BPA.[135] There are also examples wherein common photoinitiators are synthesized as aryl diazonium salts for electrografting on gold electrodes. Using this approach, Khlifi et al.[140] and Gam-Derrouich et al.[141] were able to produce melamine and dopamine-imprinted MIP sensors via electrografting of the photoinitiator and subsequent surface-initiated polymerization. Upon immersing the electrode in a pre-polymerization mixture including the template, methacrylic acid (MAA) as a functional monomer, ethylene glycol dimethacrylate (EGDMA) as a cross-linker and a mixture of methanol-chloroform as solvent, they achieved a rapid and facile grafting of MIPs onto the gold surface by exposure to 365-nm UV light.

Another example was reported by Ton et al. who used a conventional telecommunication optical fiber to direct a 375-nm UV laser beam into a drop of a precursor solution directly suspended at the end of the fiber. This resulted in the formation of a MIP microtip directly interfaced with the

optical fiber (Figure 4). This sensor allowed detecting the fluorescent target dansyl-phenylalanine based on a bifurcated setup allowing for separate excitation and detection, and also the non-fluorescent target 2,4-dichlorophenoxyacetic acid when a fluorescent reporter monomer was included into the MIP.[137] It should be mentioned here that UV light of shorter wavelengths (e.g. 312-nm) has been shown to self-initiate the polymerization of acrylic monomers,[139] which allows for the initiator-free synthesis of MIPs, as reported for instance by Panagiotopoulou et al. These monomers achieve a triplet state upon UV absorption (≤312 nm), which leads to either biradical formation or hydrogen abstraction.[134,142] UV photopolymerization has also been used for more conventional MIP formats such as microparticles,[143] films[133,144] and membranes.[145]

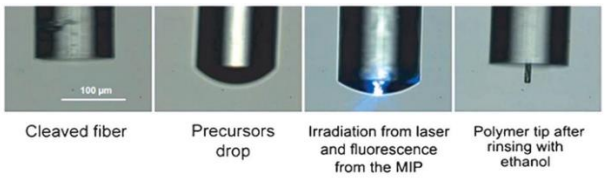

Figure 4. The fabrication process of an imprinted microtip by guiding UV through an optical fiber to the MIP precursor drop. Reproduced with permission from ref 137, copyright 2013 Wiley-VCH Verlag GmbH & Co.

UV-A photopolymerization of MIPs can also proceed *via* controlled radical polymerization. As mentioned above, controlled radical polymerization allows controlling the molecular weight of growing chains, and provides access to block copolymers *via* chain-extension of polymers, which behave as macro-initiators ('living character'). It has also been shown that binding capacity and binding affinity may be improved compared to classical FRP, through an improved network

structure.[27] Nevertheless, its main advantage over the latter technique is the chain-extension capability, which allows tuning the chemistry and reactivity of the MIP surface.[27]

Photoiniferter polymerization was the first controlled polymerization technique applied to the synthesis of MIPs in 1997 by Wang et al.[27] A great majority of photoiniferters used for MIPs rely on benzyl-derived dithiocarbamates and require an excitation near 365 nm.[92,93,146–148] For instance, the iniferter diethyldithiocarbamate (DEDTC) was exploited by Kidakova et al. to control the thickness of MIP growth in combination with microcontact printing for the imprinting of bovine serum albumin (BSA). A chlorinated diazonium salt was electrochemically reduced onto a gold substrate for grafting DEDTC on the surface. Meanwhile, BSA was immobilized on a separate glass slide via an epoxy-silane linker. An aqueous precursor solution consisting of 2-(diethylamino)ethylmethacrylate (DEAEM) and MBAAm was sandwiched between the DEDTC-modified gold substrate and the BSA-modified glass slide before exposure to 365-nm UV light. After peeling off the glass slide bearing the BSA molecules, the resulting thin MIP on the gold substrate allowed sensing the protein by surface plasmon resonance (SPR). The sensor displayed a rather narrow dynamic range between 2.5 nM and 25 nM and an adsorption capacity for BSA only twice that of similar proteins (i.e. human serum albumin and the Fc fragment of immunoglobulin G), indicating limited selectivity.[131]

RAFT polymerization is one of the most popular controlled radical polymerizations and operates with a chain transfer mechanism similar to that of iniferter. There are no examples on photo-RAFT polymerization of MIPs in the UV range, most examples using visible light, as outlined below. Some papers still refer to photo-RAFT even though no external radical source is involved: in these cases, a RAFT agent is irradiated with UV light thus triggering its own decomposition which should be rather described as photoiniferter synthesis.[149–151]

ATRP is another widely used technique for the controlled radical polymerization of MIPs. Despite its wide success, this technique historically suffered the catalyst's incompatibility with acidic monomers such as MAA (which is arguably the most commonly used functional monomer for MIPs), which greatly limited its applicability to the molecular imprinting field. However, a breakthrough was reported in 2012, when Fors and Hawker noticed that the photocatalyst fac-[$Ir(ppy)_3$] could tolerate MAA much better than previous catalysts, making possible the synthesis of PMAA of around 30 000 kDa with a PDI as low as 1.61.[100] Taking advantage of the robustness of fac-[$Ir(ppy)_3$], Adali-Kaya et al. thus reported on the synthesis of MIPs specific for S-propranolol and testosterone, both formulated using MAA as functional monomer. Two different formats were tested (i.e. bulk and nanoparticles) which in both cases afforded MIPs with affinities and selectivities comparable to those of similar MIPs obtained by FRP. In addition, the halide-capped chain-ends allowed for chain-extension and grafting of polyacrylamide p(AAm) brushes onto MIP nanoparticles.[81]

II.5.2. Visible and NIR light mediated photopolymerization of MIPs

There is currently a growing interest in the use of visible light for photopolymerization in the MIP field due to its considerable advantages over conventional UV polymerization. The lower energy of visible light allows for more specific light-induced processes. As opposed to UV radiation, visible light is less likely to alter the ingredients of the MIP precursor mixture other than to initiate polymerization. Moreover, the now widely available LEDs as visible-light sources generate less heat and thus help avoiding thermal effects on polymerization.

Urraca and co-workers exploited for instance a system composed of Eosin Y and methyldiethanolamine as a Type II initiator to synthesize a MIP using a 532-nm green laser. To

do that, they coated an aluminum film featuring nanoholes laid on top of a glass substrate with a precursor mixture containing the initiating system, the template rhodamine 123, MAA, the crosslinker EGDMA and acetonitrile (ACN). The laser beam was then directed onto the glass slide to synthesize sub-micron MIP dots for the fluorescent assay of rhodamine 123.[96] Wei's group chose a photo-redox couple sensitive to red light based on methylene blue/*p*-toluenesulfinate for the surface functionalization of SPR chips with theophylline-imprinted polymers. The aqueous pre-polymerization mixture composed of the template, MAA, MBAAm and the photo-redox initiator system was sandwiched between an SPR gold chip and a cover glass which was peeled off after polymerization. Irradiating with a red laser beam of 633-nm wavelength resulted in the formation of a MIP for theophylline.[152] There are only very few Type I visible-light photoinitiators with wavelengths above the blue region, one of them being the titanocene initiator at 532 nm (Table 1).[138]

As mentioned above, an interesting route for visible-light driven photopolymerization consists in using the emission of fluorescent nanoparticles upon excitation with shorter or longer wavelengths. Panagiotopoulou et al. used two kinds of QDs to locally grow a MIP shell around them by excitation with UV in the presence of visible-light-active, Type II photoinitiators (Figure 5) set off by the fluorescent light of the QDs. Since the light intensity emitted by the QDs decreases with distance, polymerization only took place in close proximity to the QDs. In their experiment, they used InP/ZnS QDs (red and green emitting QDs) combined with two photo-initiating systems: respectively a methylene blue/trimethylamine (TEA) and an Eosin Y/TEA tandem. Thus, after growing a first hydrophilic shell based on poly[2-hydroxyethylmethacrylate-co-N,N'-ethylene bis(acrylamide)] by irradiating with 365-nm UV light, they then synthesized thin MIP shells imprinted with N-acetylneuraminic acid (NANA) on red emitting QDs and glucuronic acid (GlcA)

on green emitting QDs as a second layer. Thanks to the embedded emission properties of the resulting imprinted composites, both red and green MIP-coated QDs were applied as biocompatible imaging agents for the multiplexed detection of glycosylations in cells.[128] The same principle was employed to synthesize thin MIP shells directly around carbon dots (CDs),[153] and very recently, around individual protein molecules. The latter was possible by using proteins (myoglobin, lactoferrin) surface-derivatized with Eosin, as macroinitiators. After removal of the template protein, the resulting nanogel particles contained on average one binding site and specifically recognized their target protein.[154]

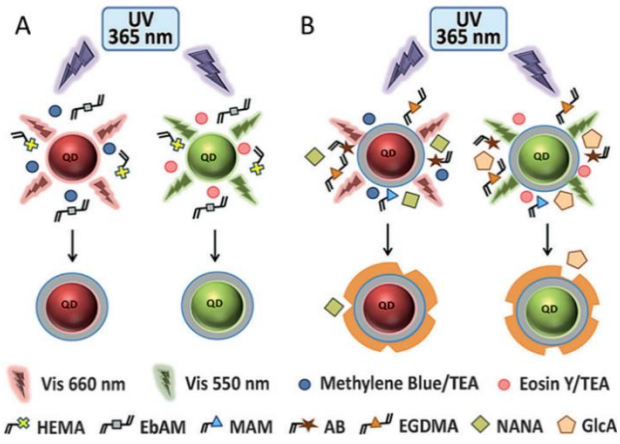

Figure 5. General scheme for the synthesis of a polymer shell around red and green InP/ZnS emitting QDs. Excitation with UV light allows sequentially polymerizing (A) a hydrophilic shell, and (B) the MIP layer. Reproduced with permission from ref. 128, copyright Wiley-VCH Verlag GmbH & Co.

The first example of molecularly imprinted nanocomposites synthesized by upconversion of NIR light was reported by Beyazit et al. who demonstrated a general strategy for coating the

$NaYF_4:Yb^{3+},Er^{3+}$ UCPs with a polymer layer. Oleic acid-stabilized UCPs were immersed in a toluene/DMSO solution containing HEMA, EbAM, and N-acryloyl-p-aminobenzamidine·HCl (AB) as monomers and Eosin Y/TEA as photoinitiator for growing a MIP. Upon exposure to 980-nm NIR, the UCPs emitted visible light between 520-540 nm, which allowed polymerizing first a hydrophilic polymeric shell around the particles. Similarly to the case of QDs, the light intensity emitted by UCPs decreases with distance, which confines the polymerization close to the surface, thus affording thin layers. The hydrophilic UCPs were subsequently dispersed in phosphate buffer containing new monomers, and a second (MIP) shell was synthesized using trypsin as a template. In this way, the AB monomer included in the first shell was used to anchor the template for the synthesis of a second, imprinted shell. Measurements with fluorescein isothiocyanate-labelled trypsin showed that the UCP-MIPs were selective for trypsin over other serine proteases such as kallikrein and thrombin.[70] In a similar context, NIR can be upconverted to blue and even near UV light and used to locally trigger photopolymerization (see previous section).[70] In this perspective, Gou's team reported using a 'bioink' consisting of UV-sensitive photoinitiator-coated UCPs and gelatin methacryloyl for the subcutaneous *in vivo* polymerization of projected NIR constructs.[155] The $NaYF_4$:Yb,Tm-based UCPs upconverted 980-nm NIR into UV light between 340 nm and 375 nm allowing the photoexcitation of lithium phenyl-2,4,6-trimethylbenzoylphosphinate that was previously electrostatically adsorbed on the positively charged UCPs. Since NIR can penetrate the skin tissue, subcutaneous injection of the bioink into mice and the subsequent exposure of the injected area to NIR constructs resulted in the polymerization of triangular, cross-shaped and double-layered microstructures. The application was further extended to the *in vivo* polymerization of ear-like tissue and scaffold for muscle defect repair by adding chondrocytes and adipose-derived stem cells, respectively, to the bioink formulation. In all cases, there were no apparent adverse

effects to the surrounding tissues nor to the vital organs studied for a period up to a month. The work served as a proof-of-concept for non-invasive *in vivo* 3D bioprinting with the aid of UCPs.[155] In another example, Tang et al. fabricated core-shell MIP nanoparticles based on the UCP $NaYF_4:Yb^{3+},Er^{3+}$ that would serve as fluorescent probes for sensing quinolones in fish samples (Figure 6). The UCPs were first coated with an ultrathin silica shell doped with Fe_3O_4 to render it magnetic for easy handling. They were then added to a MIP precursor composed of the template enrofloxacin (ENRO), MAA, EGDMA and benzophenone in dichloromethane (DCM)/TEA. The setup was exposed to a 980-nm infrared radiation, upon which the UCPs emitted light mainly at 405-nm, triggering the formation of the MIP layer on the surface. The resulting MIP UCPs were able to detect and measure ENRO together with other quinolones since these target molecules, through their hydrogen bond with the functional groups found in the binding sites, could quench the fluorescence of the MIP UCPs when exposed to 980-nm NIR. The MIP UCPs exhibited fast response, high selectivity and specificity towards five quinolones.[132]

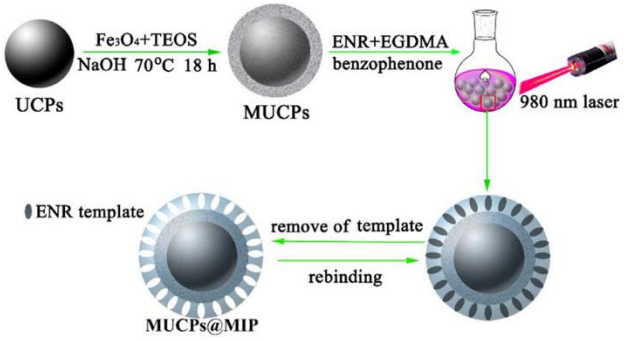

Figure 6. Schematic representation of the fabrication of the MIP magnetic upconverting particles (MUCP). Reproduced with permission from ref. 132, copyright 2018 Elsevier B.V.

Over the last few years, visible light has also been used to trigger controlled radical polymerizations in the MIP field, using photoiniferters, RAFT and ATRP. Garcia-Soto et al. reported for instance on the first use of 4-cyano-4-[(dodecylsulfanylthiocarbonyl) sulfanyl]pentanoic acid (CDTPA) as a photoiniferter under low-power visible light. CDTPA allowed polymerizing MIPs for testosterone by irradiating the prepolymerization mixture with either a blue (435-nm) or green (520-nm) LED. The resulting microspheres showed similar affinity for the template, albeit the size was smaller for the MIP synthesized at the shorter wavelength, which was related to the different extent of activation reached upon irradiation.[95]

Only one example of MIP obtained by visible-light RAFT polymerization has been reported. Zhu et al. used TPO-L as radical source at 420 nm and 2-(((ethylthio)carbonothioyl)thio)-2-methylpropanoic acid (EDMAT) as RAFT agent.[156] The MIP imprinted with glucose was intended for glucose sensing in urine samples. Apart from that, the tandem PET-RAFT has been applied to the visible-light photopolymerization of MIPs, as shown by Cai et al. who grew a melamine-imprinted layer on gold nanoparticles (AuNPs) for electrochemiluminescence (ECL)-based sensing. The strategy involved the electrostatic adsorption of $Ru(bpy)_3^{2+}$, a water-soluble PET catalyst and a typical ECL reagent, on negatively charged, citrate-stabilized AuNPs, and then the dispersion of such particles in a precursor mixture consisting of the template (melamine), MAA, EGDMA and the RAFT agent 4-cyano-4-ethyltrithiopentanoic acid (CETP) in an ethanol/water solution. Polymerization on the surface of the Au aggregates was achieved by triggering the PET process with 465-nm blue light. The hybrid MIP was further mixed with Nafion to form a composite that was later deposited on a highly ordered pyrolytic graphite (HOPG) substrate. The resulting sensor could detect melamine over a wider concentration range compared, for instance, to silica and multiwalled carbon nanotubes, while showing similar LODs. This advantage was

attributed to the properties of AuNPs such as good conductivity, large surface area available for ECL by $Ru(bpy)_3^{2+}$ and the LSPR phenomenon.[157]

II.6. Limitations of photopolymerization of MIPs

Despite the obvious advantages mentioned above, photopolymerization has also a number of limitations, both in general and from a MIP point of view. General limitations are more of the technical kind, such as the limited penetration depth of light into bulk solutions and suspensions (physical barrier). This is dependent on the wavelength (visible light usually penetrates better than UV), and may require special reactor designs to ensure homogeneous irradiation and high polymerization yields. As a result, photopolymerization has been more widely adopted to the synthesis of micro and nanostructures and to the patterning of polymers, than to the synthesis of bulk materials.

Specifically in the MIP field, there are a number of additional factors to be taken into account. Since most organic molecules absorb at least UV light, the template molecule used to generate the MIP may be sensitive to the irradiation during photopolymerization, in particular with UV initiators. On the other hand, photopolymerization at higher wavelengths of the visible spectrum mostly use Type II photoinitiators (a notable exception being the titanocene initiator at 532 nm[138], see Table 1). These require a co-initiator (often an amine), which renders the polymerization solution more complex and may even interfere with the template-monomer assembly.

III. Photostructuring MIPs

The different means of tuning a photopolymerization (i.e. spatiotemporal, wavelength, intensity, pulsating) make this process a favorable strategy for the structuration of polymers and their

intelligent design and engineering into arbitrary patterns. Adding photostructuration to molecular imprinting opens the possibility for non-contact high-resolution fabrication of micro- and nanostructures,[45,54] with applications ranging from microelectromechanical systems (MEMS), to microfluidic channels, to transducers in sensors, etc. When MIPs are structured to have dimensions in the micro-/nano-range, their effective surface-to-volume ratio increases. This allows providing a high number of binding sites with only a limited mass of MIP, which in turn improves their sensitivity, binding kinetics and binding site regeneration.[159–161] Furthermore, since light can be projected onto a surface, it also allows for an easy *in situ* polymerization of structures on substrates.[162]

Thanks to these advantages, one of the obvious applications of photo-structured MIPs deals with chemical sensing. A chemical sensor, as defined by the IUPAC, is a *"device that transforms chemical information, ranging from the concentration of a specific sample component to total composition analysis, into an analytically useful signal. The chemical information, mentioned above, may originate from a chemical reaction of the analyte or from a physical property of the system investigated*."[163] Chemical sensors are usually composed of two main functional units: a sensing element in charge of transforming the chemical information into a form of energy, and a transducer, which is responsible for translating this energy into an analytical signal. In the context of chemical sensing, it is desirable that the recognition element be optimally exposed to the sample while remaining well attached to the transducer, to effectively generate a signal upon interaction with its target. Assembling the recognition element into a structure, whether simple or hierarchical, thus needs to take into account the above requirements and is therefore a crucial step. MIPs as recognition elements offer several advantages over their biological counterparts, as they can be easily synthesized in a wide range of physical forms (e.g. bulk, micro-/nano-particles, membranes,

films, complex 2.5D and 3D elements, etc.) and interfaced on a wide variety of substrates, owing to their "synthetic" nature which also comes with superior physico-chemical properties.

III.1. Introduction to photolithography

Photolithography is a powerful technology for the fabrication of sophisticated 2D and 3D structures at the micro- and the nanoscale with the aid of light.[164] There exists a myriad of photolithographic techniques, which can be categorized into either "mask" or "maskless" techniques (Figure 7A). Conventional photolithography uses masks to transfer a pattern onto a given surface, by selectively allowing the transmission of light from a source onto a photosensitive material which is usually spread on top of a substrate. Depending on the nature of the material, the illuminated areas will either cross-link and harden, or become susceptible to removal. This is often followed by an etching step that eliminates the exceeding parts and reveals the actual pattern. Such techniques are grouped according to the placement of the mask between the light source and the photoresist into: (i) contact photolithography, (ii) proximity lithography and (iii) projection lithography (Figure 7B). Conventional photolithography is known as a "parallel" process, as it fully transfers the pattern of a mask onto a photoresist upon a single light exposure.[165,166] As such, it guarantees high throughput and high resolutions, which makes it the dominant fabrication method in microelectronics.[165,167,168] Unfortunately, photolithography can be costly as its setup often requires the use of clean rooms to prevent contamination from particulates and guarantee the quality of printed structures.[169]

The main drawback of photolithography is its diffraction-limited resolution. For proximity lithography for instance, which is carried out within the near-field (Fresnel) diffraction regime, the achievable resolution (R) is (Equation 1):

$$R \approx \sqrt{\lambda L} \qquad \text{(Equation 1)}$$

where λ is the wavelength of the source and L is the distance between the mask and the resist (usually 2-4 μm). This means that the lateral resolution for proximity lithography can be several times the used wavelength. In contact photolithography on the other hand, the mask directly touches the resist, thus bringing the resolution to the order of magnitude of the wavelength. The resolution (R) of projection lithography (and of all other lens-based lithographies) is governed by far-field (Fraunhofer) diffraction and constrained by the Rayleigh equation (Equation 2):

$$R = k_1 \frac{k}{nsin\theta} = k_1 \frac{\lambda}{NA} \qquad \text{(Equation 2)}$$

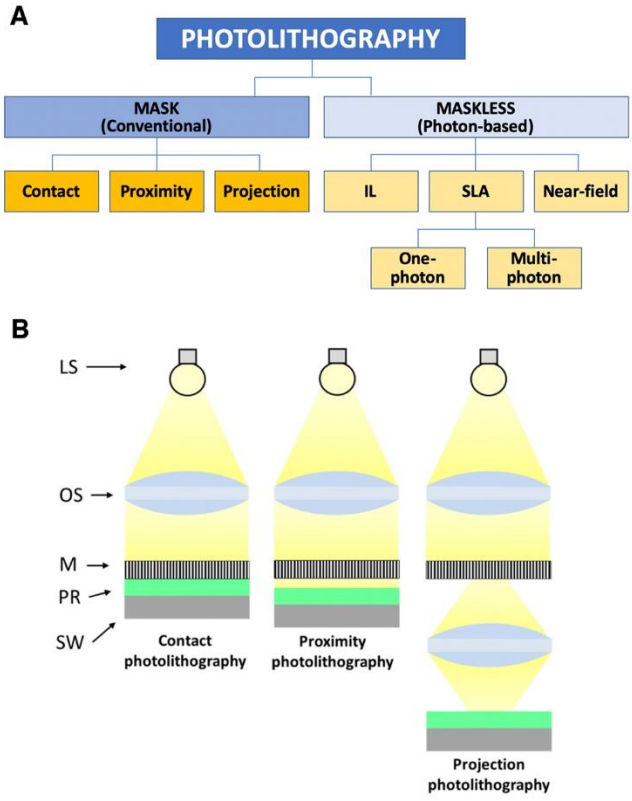

Figure 7. A: Classification of different photolithographic techniques. B: Comparison of different conventional photolithographic technique (LS=light source, OS=optical system, M=mask, PR=photoresist, SW=silicon wafer).

where "k_1" is a process-dependent factor (with values typically between 0.25 and 0.8), "n" is the refractive index of the medium, "q" is the half-aperture angle of the lens or optical imaging system used and "NA" corresponds to its numerical aperture. This places the resolution around half the wavelength of the source.[170–172] Many approaches have been developed by specifically targeting the different parameters of Equation 2 to improve lateral resolution, which afforded techniques such as deep and extreme UV lithography, phase-shift lithography or immersion lithography. As a result, resolutions down to 10 nm can now be achieved.[168,173] Deep and extreme UV lithography utilize for instance short wavelengths (193 nm and 13.5 nm, respectively). Phase-shift lithography on the other hand relies on lowering the k_1 parameter by using optically transparent masks which are micro-/nanostructured on their surface.[171,173] Such masks modify the light optical path *via* destructive interference, thus enhancing the sharpness of the replicated image. Immersing the mask projection system in a fluid with a refractive index higher than 1 (i.e. higher than air) also improves resolution as it occurs for immersion lithography.[171,174]

In contrast to the previous techniques, maskless lithography does not require any physical mask, as it relies on focusing a beam of photons or charged particles within a photoresist in order to construct patterns. Interference lithography, a photon-based technique, exploits the interference patterns of coherent optical beams incident at various angles within a photoresist. The resulting pattern may extend in 2D or 3D depending on the thickness of the reactive layer and it is generally further developed by thermal or chemical treatment in order to remove the unreacted photoresist. Also considered a "parallel" process, interference lithography represents a fast, straightforward and accurate approach for quasiperiodic structures with resolution below 10-nm, making it attractive for fabricating photonic crystals and metamaterials.[175] Another photon-based, maskless technique is stereolithography (SLA). In SLA, a computer-generated 3D design is "directly

written" into a photoresist by focusing a laser beam of appropriate wavelength while following a sequence of stacked 2D layers which are thus photoprinted successively on top of each other by moving a "z" stage. SLA can operate via one-photon or multiphoton absorption. In one-photon stereolithography, a laser source (usually UV) is used to induce a cross-linking based on simple, one-photon absorption, as it occurs in ordinary photopolymerizations. On the other hand, multiphoton SLA (MSLA) involves the simultaneous absorption of multiple photons of low energy, which virtually matches a "single", high-energy photon absorption. A prominent example of multiphoton SLA is the two-photon stereolithography (TPS) (Figure 8). In this technique, the use of a femtosecond laser (usually with wavelengths in the NIR around 800 nm) allows for a two-photon absorption, which corresponds to the mono-absorption of a 400-nm photon. Such two-photon absorption thus allows reaching the energy threshold required to trigger the dissociation of an ordinary, near UV-active photoinitiator such as TPO-L. Many works have been dedicated to develop specific photoinitiators exhibiting a high two-photon absorption cross-section. Unlike one-photon stereolithography, MSLA has the advantage of being exclusively confined within the (small) focal point of the beam (i.e. less than 1 μm^3) where high intensities promote a two-photon absorption process (Figure 8B). Thus, multiphoton SLA enables a highly localized polymerization of the photoresist, which is essential for the direct writing of elaborate 3D geometries (Figure 8D). However, multiphoton SLA only affords a resolution of a few hundred nanometers and provides a low throughput as it belongs to "serial" processes, which operate with a multi-exposure to light for the voxel-to-voxel printing of the resist.[165,166] Nevertheless, MSLA is compatible with a wide variety of photoresists including (meth)acrylates, epoxides, organically modified silica and organically modified ceramics.[175–177]

While the lateral resolution for traditional TPS can be as small as a few hundred nanometers, successful attempts have been made to reduce this value by modifying the experimental setup. For instance, Gan et al. relied on the use of a second laser beam around the focal point of the primary laser source for the activation of a photoinihibitor to limit the polymerization and reduce the lateral writing resolution to 52 nm and a record feature size of 9 nm.[178] Haske et al. on the other hand

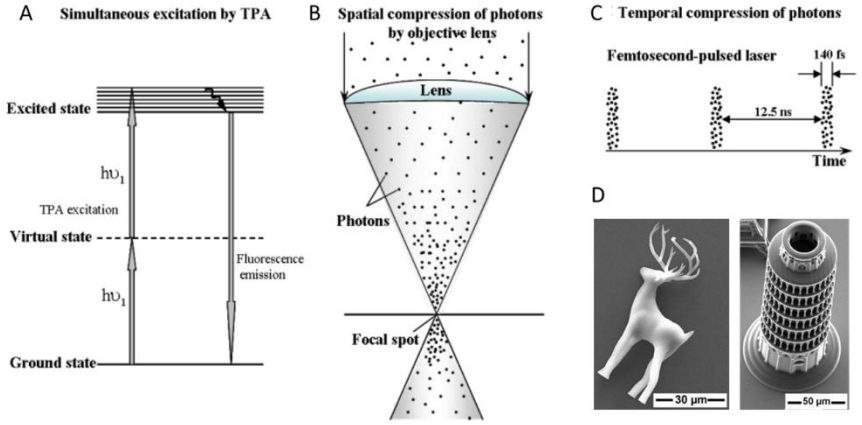

Figure 8. (A) Jablonski diagram showing electronic excitation via two-photon absorption. (B-C) Spatial and temporal compression of photons for increasing the probability of two-photon absorption. Reproduced with permission from ref. 179, copyright 2013 IntechOpen. (D) Representative SEM images of microstructures with complex geometries printed via TPS.

reduced the resolution based on the Rayleigh equation (Equation 2) by using a 520-nm laser source whose dosage had been optimized against a resist containing the photoinitiator DABP.[180] Jiang et al. took advantage of polythiols to provide a photoresist with oxygen tolerance as well as to expand the writing range, while enabling the use of near-threshold laser dosages for the production of mechanically stable fine lines.[181]

A different approach was instead used by Liu and co-workers, who deliberately fabricated photonic woodpiles with an intralayer rod distance of 1.57 μm which decreased to 350 nm by thermal-shrinking at 450°C, resulting in the appearance of a visible color due to the woodpiles.[182]

Defying the diffraction limit, near-field-assisted optical lithography may also be included among light-based lithography techniques, which can be used in different configurations, including mask and maskless approaches. This technique triggers a polymerization using the evanescent wave which can be generated in different configurations. By its nature, the optical near-field is not governed by the classical diffraction limit, which permits to reach high resolution (down to the lower nm scale using visible light). Total internal reflection of light at the interphase between two media with different refractive indices and which propagates into the medium of lower index can be used to generate near-field irradiation.[183] This technique allows for a highly confined polymerization (i.e. few tens of nm), as the energy of the evanescent wave which tails from the interphase decays exponentially.[184,185] Metal nanostructures excited in their resonance plasmonic bands are also very interesting to generate near-field excitation with nanoscale resolution, as described in several examples.[186–188] The near-field being generated at the surface of the metal structure, in hot-spots, this method is quite efficient to couple polymer materials with metal nanostructures, with a precise control of the polymer position in proximity of the nanostructure.[189]

Finally, maskless techniques can also rely on charged particles, such as electron-beam lithography (EBL) and focused-ion-beam lithography (FIBL). In EBL, a beam of accelerated electrons is scanned on the surface of a resist, such as polymethylmethacrylate (PMMA), in order to alter its solubility. Upon development, a pattern is created in the resist, which can in turn be transferred to a substrate upon further etching. FIBL is analogous to EBL but it applies an accelerated beam of ions, such as He^+ and Ga^+. FIBL can also be used to deposit materials such as

tungsten, platinum and carbon on a surface. This is typically achieved upon interaction between a focused ion beam and a gaseous precursor in proximity to a surface, wherein the precursor decomposes.[190] EBL and FIBL can achieve high resolutions, with features below 10 nm, but they remain costly and rather difficult to miniaturize. Similarly to SLAs, they also have low throughputs.[168,171] Representative examples of the above techniques triggered by light and applied to the synthesis or functionalization of MIPs will be discussed in the following paragraphs.

III.2. Mask lithography of MIPs

III.2.1. *Contact and proximity photolithography*

A straightforward technique for photostructuring MIPs is contact lithography. Contact photolithography involves the use of a photomask touching the surface of a photoresist. Upon irradiation with a suitable wavelength, the exposed zones of the resist undergo polymerization, which results in transferring a pattern from the mask to the underlying polymer (i.e. MIP). This approach involves the use of what is called a negative tone resist, which upon washing with a "developing" solution affords polymeric structure features as the inverse pattern of the mask. Similarly, positive tone resists also exist, which work in the opposite way, i.e. the exposed zones become soluble and can be removed with the developing solution. Despite being conceptually simple, contact photolithography requires a complete and direct contact between the resist and the photomask to avoid defects and contamination, but this can sometimes be particularly tricky. To avoid such mishaps, proximity printing can be used, which overcomes the above limitations by including a small gap between the resist and the mask during the photostructuring step (Figure 7B). The gap must be as small as possible to preserve the resolution but big enough to prevent defects and contamination.

Ayela's group has pioneered contact photolithography of MIPs, at the wafer scale, fabricating consecutively multiplexed patterns of different MIPs on the same silicon wafer, with a μm resolution. This was done by UV photopolymerization of spin-coated monomer films under nitrogen atmosphere, using standard photolithography equipment with a mask aligner.[191] More recently, Hearn and co-workers applied contact lithography to the synthesis of a double-layered MIP thin film in the form of a grid-patterned surface, with the aim of developing a tool for the direct and visual comparison of different functional monomers toward the binding of the fluorescent target N-dansyl-L-phenylalanine (Figure 9A).[192] Their strategy relied on the spin-coating and curing of two consecutive prepolymerization mixtures based on different functional monomers: first, a formulation based on methacrylic acid (MAA, i.e. MIP1), then a second based on 4-vinyl pyridine (4-VP), with N-boc-L-phenylalanine as a non-fluorescent template analogue in both cases. The spin-coated formulations were both cured at 365 nm, but only for the second one a 300-mesh TEM gold grid was used as a mask, which resulted in a double layered MIP system consisting of a series of patterned squares (MIP2) on top of a continuous film (MIP1). Upon incubation with N-dansyl-L-phenylalanine, fluorescent microscopy images revealed that the squares had a much higher fluorescent intensity than the underlying film (Figure 9B), thus suggesting that 4-VP had a higher affinity for the target, as supported by molecular modelling and ^{1}H NMR spectroscopy titrations.

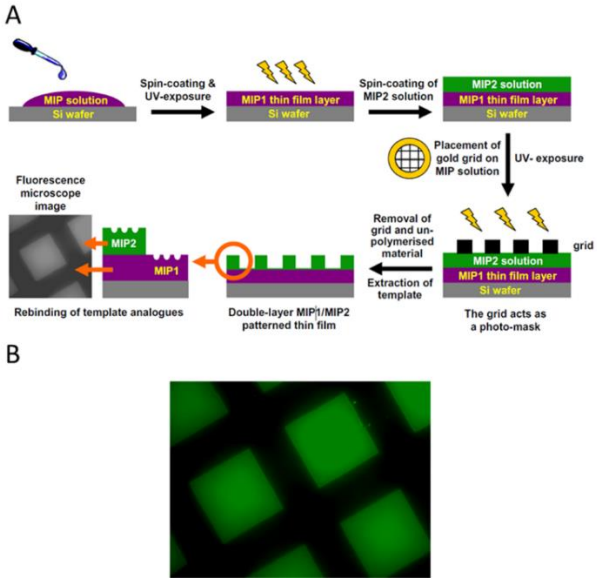

Figure 9. (A) Schematic representation for the preparation of a grid-patterned double-layered MIP2/MIP1 thin film by contact lithography. (B) Fluorescence microscope image of a grid-patterned double-layer MIP1/MIP2 thin film with the 54 µm x 54 µm raised MIP2 squares selectively binding the fluorescent target N-dansyl-L- phenylalanine. Reproduced with permission from ref. 192, copyright 2012 Elsevier B.V.

In another work, Liu's group fabricated thin-film arrays on a pre-treated glass slide or filter membrane by light-curing a pre-polymerization solution while covering it with a patterned photomask. The MIP was based on boronic acid as functional monomer, which is known to interact with cis-diols such as present in certain sugars via reversible covalent bonds. These imprinted arrays were used for the colorimetric detection and chemiluminescent assay of five glycoproteins, with the test exhibiting a limit of detection as low as 1 ng mL^{-1} for one of the glycoproteins.[193]

More recently, Nicu and his team integrated MIPs into arrays of nanocantilevers (Figure 10) for a label-free detection via functionalized resonators.[194] To achieve this, a 100-mm silicon-on-

insulator (SOI) wafer was dry-etched to shape a cantilever and silanized with 3-(trimethoxysilyl)propyl methacrylate to anchor an organic MIP. The cantilever was then spin-coated with a monomer mixture and placed under an automatic mask aligner for photolithography. Upon photopolymerization and wet etching of the sacrificial oxide layer, a MIP coated cantilever was obtained which worked as a nanoelectromechanical system (NEMS) for sensing the fluorescent N-dansyl-L-phenylalanine. Preliminary results showed that while the mechanical sensing on cantilevers required further optimization due to the damping by the polymer, a direct fluorescence measurement of the target confirmed a successful imprinting, with the MIP cantilever emitting about 3.5 times stronger fluorescence intensity than the corresponding NIP cantilever.

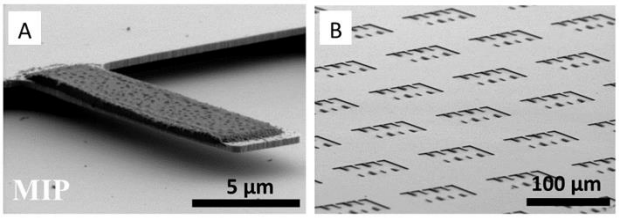

Figure 10. SEM images of (A) a MIP-coated silicon cantilever obtained by photolithography and (B) large-scale arrays of MIP cantilever. Reproduced with permission from ref. 194, copyright 2019 IOP Publishing.

III.2.2. *Projection photolithography*

In projection photolithography, the photomask is placed at a certain distance from the resist while an optical system is located in between to focus the pattern image from the mask onto the resist (Figure 7B). In this way, it is possible to overcome the mechanical and diffraction issues encountered in contact and proximity photolithography, which improves the whole resolution. For instance, Haupt's group combined microscope projection photolithography with nanomolding to

prepare arrays of MIP nanofilaments (Figure 11A-B) by inserting a photomask into the field-diagram plane of a microscope. In this way, UV light from the mercury lamp of the microscope could pass through the unmarked areas of the mask and polymerize 70 nm-dots from a methacrylate-based precursor solution. The light was also filtered with an IR mirror to prevent thermal polymerization. Since the precursor was deposited on a nanoporous alumina substrate, the polymerized spots were composed of upright MIP nanofilaments (Figure 11C-E) whose structure provided a large surface area and an easy diffusion of the targets fluorescein or myoglobin. This approach also allows decreasing the size of the projected pattern (i.e. the size of the dots) by simply using higher magnification objectives, as well as improving the whole resolution by using higher numerical apertures.[195]

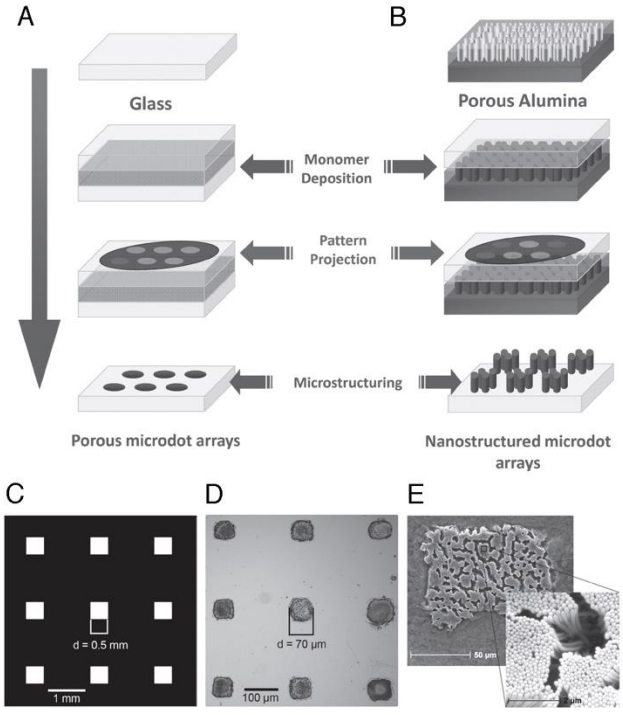

Figure 11. Schematic representation of the preparation of (A) porous microdot arrays and (B) nanofilament microdot arrays by microscope projection photolithography. (C) Transparent

photomask. (D) Bright-field microscopy image of the polymer array obtained using the photomask by projection photolithography. (E) SEM image of a single nanofilament dot (magnification: 750 x, inset: 20000 x). Reproduced with permission from ref. 195, copyright 2011 Wiley-VCH Verlag GmbH & Co. KGaA.

III.3. Photon-based, maskless lithography

III.3.1. *Interference lithography*

Among the techniques that manipulate lasers for direct writing, holographic lithography or multibeam interference lithography (MBIL) consists of two or more non-parallel laser beams directed into a photoresist to trigger a polymerization according to their interference pattern.[196] An example of MBIL MIP writing was reported by Fuchs et al., who imprinted testosterone as template using MAA and pentaerythritol triacrylate (PETA) as monomers and bis(cyclopentadienyl)titanium dichloride as green light-sensitive radical initiator. Upon laminating this formulation between two microscope glass slides, one of which functionalized with double bonds for a better MIP adhesion, a coherent 532-nm laser beam was split into two components, which were later converged into the precursor mixture to polymerize a MIP. (Figure 12A). This resulted in well-defined diffraction gratings (Figure 12B-C), able to sense the presence of testosterone by varying their diffraction efficiency.[138]

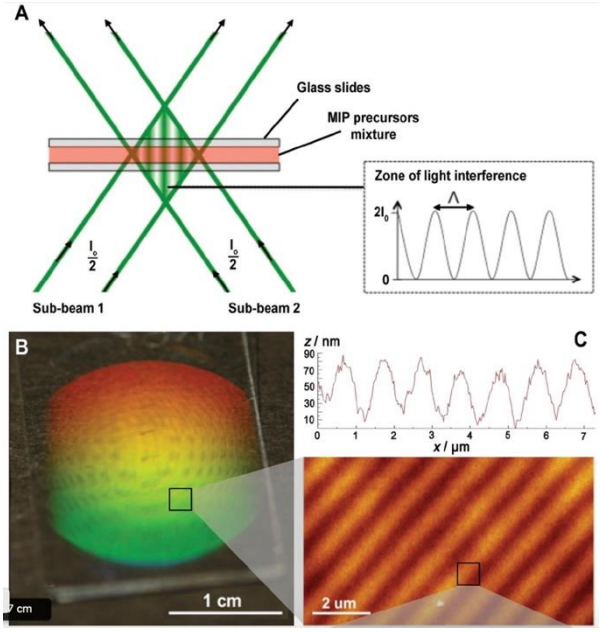

Figure 12. (A) Scheme showing the *in situ* MIP microstructuring process by interference lithography with two laser beams at 532 nm. (B) Holographic MIP film supported on a glass slide. (C) AFM image of the surface topography of a holographic MIP film (10 µm × 10 µm). Reproduced with permission from ref. 138, copyright 2013 Wiley-VCH Verlag GmbH & Co. KGaA.

III.3.2. *One-photon stereolithography*

Microstereolithography (µSL) is another approach for fabricating 3D structures by localized photopolymerization using a sharply focused laser beam. A 3D model of the desired shape is initially sliced into consecutive 2D layers by a computer-aided design (CAD) program. A laser beam of the appropriate wavelength is then focused in a precursor solution a few micrometers above a microscope slide to write the first 2D layer. This allows minimizing light scattering, for an improved resolution, while also preventing a premature polymerization of the second 2D layer.[177,197,198] The motion of the substrate along the z-axis then allows the structure to grow to 3D.

Shea and co-workers were the first to use this technique for MIPs, manufacturing 600 μm x 600 μm 2D and 3D (today considered 2.5D) grids (Figure 13) imprinted with 9-ethyladenine using a 364-nm Ar+ laser and an x-y-z motorized stage to explore the possibilities of miniaturization, which is important in sensing and diagnostics as it limits both energy consumption and production costs. Recognition of the target 9-dansyladenine was evaluated through a fluorescence assay which showed that the MIP grids had affinity for the target comparable to bulk MIPs.[162,199]

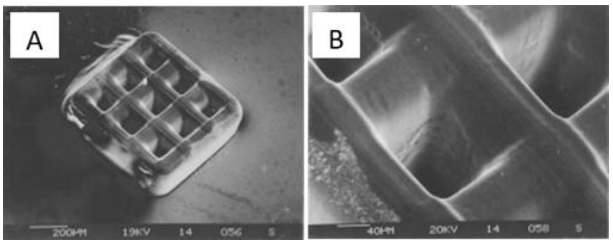

Figure 13. (A) SEM image of a 3D imprinted microstructure (600 μm x 600 μm x 100 μm) fabricated by microstereolithography. (B) Magnification of the structure showing a wall thickness of around 10 μm. Reprinted with permission from ref. 199, copyright 2003 Wiley-VCH Verlag GmbH & Co. KGaA.

III.3.3. *Multiphoton stereolithography*

The MIP photostructuring methods described so far were based on single-photon absorption. However, as outlined in section 3.1, fabrication of 3D structures by multiphoton stereolithography has recently gained great attention. Multiphoton stereolithography (MSLA) relies on a multiphoton absorption process highly confined within the focal volume of a laser beam passing through a microscope objective. It is therefore a true 3D fabrication approach since complex structures can be manufactured by moving the laser focus in three dimensions. The best-known example is two-photon stereolithography (TPS). The use of TPS in molecular imprinting is relatively new, even

though the technique has already been reported in several different applications such as scaffolding for cells,[200,201] shape-shifting of microstructures for proteins,[202] biocompatible hybrid materials,[203] tomography,[204] and optics.[205,206] This technique was first applied to the synthesis of MIPs by Chia Gomez et al., who showed its versatility by fabricating different structures such as grids, dot arrays and cantilevers smaller than 60 µm (Figure 14). Lucirin TPO was used as a photoinitiator for a laser wavelength of 800 nm. An array of dots forming the words MIP (imprinted dots, with Z-L-Phe as template) and NIP (non-imprinted dots) were for instance printed, which upon incubation with a fluorescent template analogue (i.e. dansyl-L-Phe) only emitted green light in the case of the MIP (Figure 14B). Interestingly, MIP cantilevers, a format which normally requires time-consuming and multi-step processes to be made, were also conveniently fabricated by TPS and allowed the straightforward sensing of their target Z-L-Phe as shown by a frequency shift exquisitely limited to the MIP (Figure 14D). [122,179,196,207]

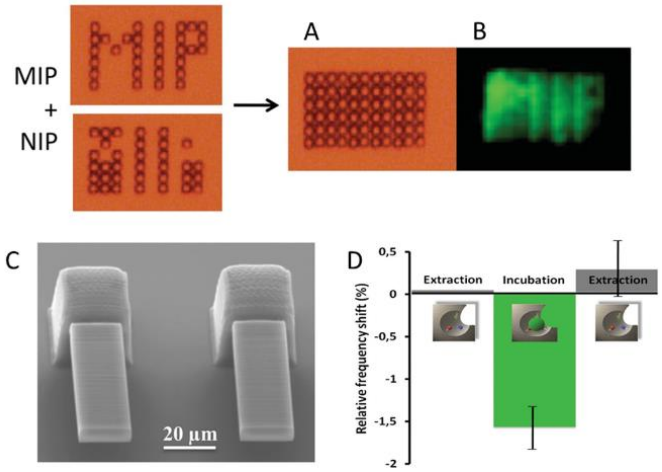

Figure 14. (A–B) Multiplexed NIP and MIP dots polymerized on the same sample by two-photon stereolithography (TPS): (A) Optical and (B) fluorescence microscopy images after binding of dansyl-L-Phe. (C) SEM images of MIP cantilevers fabricated by TPS. (D) Relative frequency shift

of MIP microcantilevers after extraction, incubation in Z-L-Phe and second extraction. Reprinted with permission from ref. 122, copyright 2016 Wiley-VCH Verlag GmbH & Co. KGaA.

III.3.4. *Near-field assisted optical lithography*

Photolithographic techniques that rely on optical lenses are based on far-field optics, and as we previously mentioned, their resolution is limited by the Rayleigh resolution and the out-of-focus light. This means that current optical equipment allows resolution between λ/2 to λ. Near-field optics, on the other hand, circumvent this problem by taking advantage of optical phenomena such as evanescent waves, which occur between the probe and the sample at sub-wavelength distance.[208,209] It should be stressed here that the evanescent wave features the same wavelength as the reflected radiation. Polymerization by evanescent wave (PEW) was first applied to MIPs by Fuchs et al. who fabricated ultrathin microdots imprinted against the template Z-L-Phe by using MAA, 4-VP and EGDMA as monomers in acetonitrile (ACN) and the initiator Irgacure819. The low-refractive index precursor solution was interfaced with a high-refractive index glass slab carrying a prism of the same index (Figure 15A). An actinic laser of 405 nm was internally reflected within the prism-slab system, allowing for the evanescent wave at the slab-precursor interface to initiate polymerization, leading to microdots of sub-100 nm thickness (Figure 15B-E). The MIP microdots showed selectivity and some degree of enantiospecificity toward their target, dansyl-D-phenylalanine. The method allowed for quick fabrication (within tens of seconds) of MIPs as thin as <100 nm.[183]

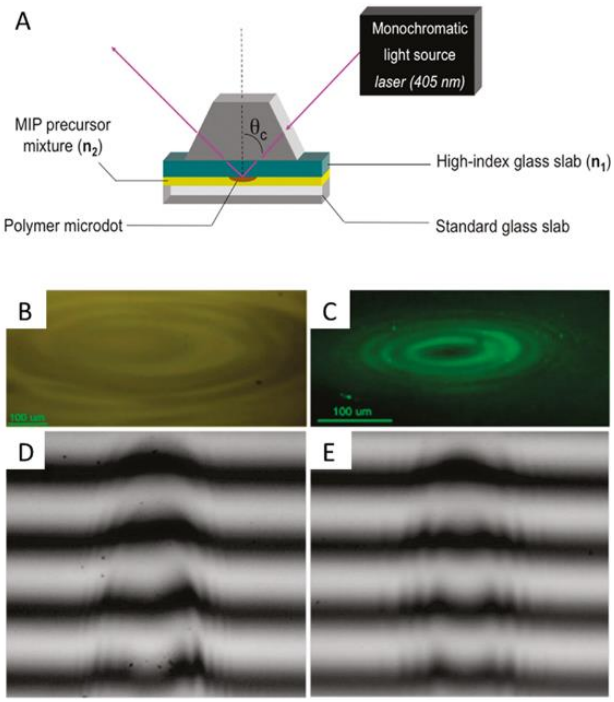

Figure 15. (A) Schematic representation of the setup for the polymerization of MIP microdots by evanescent wave. (B) Optical microscope image (20 x) of a MIP microdot. (C) Fluorescence microscope image (20 x) of a MIP microdot. Interferential microscopy images of (D) a MIP microdot and (E) a NIP microdot. Reproduced with permission from ref. 183, copyright 2011 American Chemical Society.

IV. Conclusions

From the synthetic point of view, MIPs are compatible with a variety of structuring techniques, particularly with photon-based lithographic approaches as we presented in detail in this review. These techniques allow not only fabricating micro- and nano-structures with high capacity and sensitivity, due to favorable surface-to-volume ratios, but also shaping and pattering MIPs for

generating a direct, analytical signal upon binding, which is essential for some applications such as sensing.

Each photon-based lithographic technique has its own strengths and weaknesses and this review is intended to help the reader to make his choice depending on his purpose. With its high-throughput and the different possibilities of improving resolution, conventional photopolymerization and photolithography are expected to continue flourishing in MIP fabrication. Focusing on the light sources associated with these techniques, a great majority of them use UV light to trigger the polymerization, but longer wavelengths such as visible and NIR are gaining attention in MIP synthesis, as they are more suited for processing mixtures containing sensitive templates such as bio(macro)molecules and are inherently safer.

Finally, stereolithographic techniques offer the most convenient solution to the direct writing of sophisticated architectures. Although limited by a low-throughput and rather expensive setups, stereolithography allows for direct, one-step prototyping of 2.5D and 3D structures. Among these techniques, TPS has risen as a “high-precision” technique which allows confining the polymerization to the focal point (voxel) of the used laser. Due to the multi-photon absorption process involved in TPS, NIR lasers can be used as sources to trigger near-UV or visible photoinitiators, which is advantageous when working with bio-based mixtures or even with living cells. More importantly, if strategies to improve the current TPS resolution can be standardized, it will be possible to shape materials with structural features able to rise optical properties falling directly in the visible spectrum, for a systematic tuning of molecularly imprinted optical sensors.

AUTHOR INFORMATION

Corresponding Authors

* E-mails: karsten.haupt@utc.fr, carlo.gonzato@utc.fr

Author Contributions

All authors have given approval to the final version of the manuscript. These authors contributed equally.

Notes

There are no conflicts of interest to declare.

ACKNOWLEDGMENT

The authors acknowledge the Hauts-de-France Region and the European Regional Development Fund (ERDF) (CPER 2014/2020) for the funding of equipment. EP wishes to thank the Embassy of France in the Philippines and the Commission on Higher Education of the Philippines (CHED) for granting his fellowship. KH acknowledges financial support from Institut Universitaire de France. KH and OS thank the French National Research Agency (ANR) for funding (DYNABIO grant). The authors thank Dr. Damien Thuau from the Laboratoire de L'Intégration du Matériau au Système, Université de Bordeaux, France, for help with creating the Table of Content graphics.

REFERENCES

(1) Haupt, K.; Linares, A. V.; Bompart, M.; Tse Sum Bui, B. Molecularly Imprinted

Polymers. In *Topics in Current Chemistry*; Haupt, K., Ed.; Springer-Verlag: Berlin Heidelberg, 2012; Vol. 325, pp 1–26. https://doi.org/10.1007/978-3-642-28421-2.

(2) Turiel, E.; Esteban, A. M. Molecularly Imprinted Polymers. In *Solid-Phase Extraction*; Poole, C., Ed.; Elsevier Inc., 2020; pp 215–233. https://doi.org/10.1016/B978-0-12-816906-3.00008-X.

(3) Parisi, O. I.; Ruffo, M.; Puoci, F. Molecularly Imprinted Polymers for Selective Recognition in Regenerative Medicine. In *Nanostructured Biomaterials for Regenerative Medicine*; Guarino, V., Iafisco, M., Spriano, S., Eds.; Elsevier Ltd., 2020; pp 141–163. https://doi.org/10.1016/B978-0-08-102594-9.00005-X.

(4) Cegłowski, M.; Schroeder, G. Molecularly Imprinted Polymers as Adsorbents in Mass Spectrometry Techniques. In *Comprehensive Analytical Chemistry*; Marć, M., Ed.; Elsevier B.V., 2019; Vol. 86, pp 295–336. https://doi.org/10.1016/bs.coac.2019.05.006.

(5) Polyakov, M. V. Adsorption Properties and Structure of Silica Gel. *Zhurnal Fizieskoj Khimii/Akademiya SSSR* **1931**, *2*, 799–805.

(6) Wulff, G.; Sarhan, A. The Use of Polymers with Enzyme-Analogous Structures for the Resolution of Racemates. *Angew. Chemie Int. Ed.* **1972**, *11* (4), 341. https://doi.org/10.1002/anie.197203341.

(7) Arshady, R.; Mosbach, K. Synthesis of Substrate-Selective Polymers by Host-Guest Polymerization. *Makromol. Chem.* **1981**, *182*, 687–692. https://doi.org/https://doi.org/10.1002/macp.1981.021820240.

(8) Erdem, Ö.; Saylan, Y.; Andaç, M.; Denizli, A. Molecularly Imprinted Polymers for Removal of Metal Ions: An Alternative Treatment Method. *Biomimetics* **2018**, *3* (4), 1–15. https://doi.org/10.3390/biomimetics3040038.

(9) Ardestani, F.; Hosseini, M. H.; Taghizadeh, M.; Rezaee, M. Synthesis and Characterization of Nanopore MoVI -Imprinted Polymer and Its Application as Solid Phase for Extraction, Separation and Preconcentration of Molybdenum Ions from Water Samples Fatemeh. *J. Brazilian Chem. Soc.* **2016**, *27* (7), 1279–1289. https://doi.org/10.5935/0103-5053.20160026.

(10) Perera, R.; Ashraf, S.; Mueller, A. The Binding of Metal Ions to Molecularly-Imprinted Polymers. *Water Sci. Technol.* **2017**, *75* (7), 1643–1650. https://doi.org/10.2166/wst.2017.036.

(11) Diliën, H.; Peeters, M.; Royakkers, J.; Harings, J.; Cornelis, P.; Wagner, P.; Steen Redeker, E.; Banks, C. E.; Eersels, K.; Van Grinsven, B.; Cleij, T. J. Label-Free Detection of Small Organic Molecules by Molecularly Imprinted Polymer Functionalized Thermocouples: Toward in Vivo Applications. *ACS Sensors* **2017**, *2* (4), 583–589. https://doi.org/10.1021/acssensors.7b00104.

(12) Lu, W.; Asher, S. A.; Meng, Z.; Yan, Z.; Xue, M.; Qiu, L.; Yi, D. Visual Detection of 2,4,6-Trinitrotolune by Molecularly Imprinted Colloidal Array Photonic Crystal. *J. Hazard. Mater.* **2016**, *316*, 87–93. https://doi.org/10.1016/j.jhazmat.2016.05.022.

(13) Anirudhan, T. S.; Christa, J.; Deepa, J. R. Extraction of Melamine from Milk Using a Magnetic Molecularly Imprinted Polymer. *Food Chem.* **2017**, *227*, 85–92.

https://doi.org/10.1016/j.foodchem.2016.12.090.

(14) Rossetti, C.; Ore, O. G.; Sellergren, B.; Halvorsen, T. G.; Reubsaet, L. Exploring the Peptide Retention Mechanism in Molecularly Imprinted Polymers. *Anal. Bioanal. Chem.* **2017**, *409* (24), 5631–5643. https://doi.org/10.1007/s00216-017-0520-6.

(15) Nakamura, Y.; Masumoto, S.; Matsunaga, H.; Haginaka, J. Molecularly Imprinted Polymer for Glutathione by Modified Precipitation Polymerization and Its Application to Determination of Glutathione in Supplements. *J. Pharm. Biomed. Anal.* **2017**, *144*, 230–235. https://doi.org/10.1016/j.jpba.2016.12.006.

(16) Sharma, P. S.; Iskierko, Z.; Noworyta, K.; Cieplak, M.; Borowicz, P.; Lisowski, W.; D'Souza, F.; Kutner, W. Synthesis and Application of a "Plastic Antibody" in Electrochemical Microfluidic Platform for Oxytocin Determination. *Biosens. Bioelectron.* **2018**, *100*, 251–258. https://doi.org/10.1016/j.bios.2017.09.009.

(17) Saylan, Y.; Yilmaz, F.; Özgür, E.; Derazshamshir, A.; Yavuz, H.; Denizli, A. Molecular Imprinting of Macromolecules for Sensor Applications. *Sensors* **2017**, *17* (4), 1–30. https://doi.org/10.3390/s17040898.

(18) Tchinda, R.; Tutsch, A.; Schmid, B.; Süssmuth, R. D.; Altintas, Z. Recognition of Protein Biomarkers Using Epitope-Mediated Molecularly Imprinted Films: Histidine or Cysteine Modified Epitopes? *Biosens. Bioelectron.* **2019**, *123*, 260–268. https://doi.org/10.1016/j.bios.2018.09.010.

(19) Ying, X.; Zhu, X.; Li, D.; Li, X. Preparation and Specific Recognition of Protein

Macromolecularly Imprinted Polyampholyte Hydrogel. *Talanta* **2019**, *192*, 14–23. https://doi.org/10.1016/j.talanta.2018.08.084.

(20) Gast, M.; Sobek, H.; Mizaikoff, B. Advances in Imprinting Strategies for Selective Virus Recognition a Review. *Trends Anal. Chem.* **2019**, *114*, 218–232. https://doi.org/10.1016/j.trac.2019.03.010.

(21) Graham, S. P.; El-Sharif, H. F.; Hussain, S.; Fruengel, R.; McLean, R. K.; Hawes, P. C.; Sullivan, M. V.; Reddy, S. M. Evaluation of Molecularly Imprinted Polymers as Synthetic Virus Neutralizing Antibody Mimics. *Front. Bioeng. Biotechnol.* **2019**, *7*, 1–7. https://doi.org/10.3389/fbioe.2019.00115.

(22) Liang, C.; Wang, H.; He, K.; Chen, C.; Chen, X.; Gong, H.; Cai, C. A Virus-MIPs Fluorescent Sensor Based on FRET for Highly Sensitive Detection of JEV. *Talanta* **2016**, *160*, 360–366. https://doi.org/10.1016/j.talanta.2016.06.010.

(23) Ait Lahcen, A.; Arduini, F.; Lista, F.; Amine, A. Label-Free Electrochemical Sensor Based on Spore-Imprinted Polymer for Bacillus Cereus Spore Detection. *Sensors Actuators, B Chem.* **2018**, *276*, 114–120. https://doi.org/10.1016/j.snb.2018.08.031.

(24) Idil, N.; Mattiasson, B. Imprinting of Microorganisms for Biosensor Applications. *Sensors* **2017**, *17* (4), 1–15. https://doi.org/10.3390/s17040708.

(25) Hayden, O.; Lieberzeit, P. A.; Blaas, D.; Dickert, F. L. Artificial Antibodies for Bioanalyte Detection - Sensing Viruses and Proteins. *Adv. Funct. Mater.* **2006**, *16* (10), 1269–1278. https://doi.org/10.1002/adfm.200500626.

(26) Dmitrienko, E. V.; Bulushev, R. D.; Haupt, K.; Kosolobov, S. S.; Latyshev, A. V.; Pyshnaya, I. A.; Pyshnyi, D. V. A Simple Approach to Prepare Molecularly Imprinted Polymers from Nylon-6. *J. Mol. Recognit.* **2013**, *26* (8), 368–375. https://doi.org/10.1002/jmr.2281.

(27) Beyazit, S.; Tse Sum Bui, B.; Haupt, K.; Gonzato, C. Molecularly Imprinted Polymer Nanomaterials and Nanocomposites by Controlled/Living Radical Polymerization. *Prog. Polym. Sci.* **2016**, *62*, 1–21. https://doi.org/10.1016/j.progpolymsci.2016.04.001.

(28) Włoch, M.; Datta, J. Synthesis and Polymerisation Techniques of Molecularly Imprinted Polymers. In *Comprehensive Analytical Chemistry*; Marć, M., Ed.; Elsevier B.V., 2019; Vol. 86, pp 17–40. https://doi.org/10.1016/bs.coac.2019.05.011.

(29) Xie, Z.; Zhang, L.; Chen, Y.; Hu, X. Magnetic Molecularly Imprinted Polymer Combined with High-Performance Liquid Chromatography for the Selective Separation and Determination of Glutathione in Various Wild Edible Boletes. *Food Anal. Methods* **2019**, *12*, 2908–2919. https://doi.org/10.1007/s12161-019-01646-w.

(30) Hroboňová, K.; Lomenova, A. Molecularly Imprinted Polymer as Stationary Phase for HPLC Separation of Phenylalanine Enantiomers. *Monatshefte fur Chemie* **2018**, *149*, 939–946. https://doi.org/10.1007/s00706-018-2155-5.

(31) Boysen, R. I. Advances in the Development of Molecularly Imprinted Polymers for the Separation and Analysis of Proteins with Liquid Chromatography. *J. Sep. Sci.* **2019**, *42*, 51–71. https://doi.org/10.1002/jssc.201800945.

(32) Sánchez-González, J.; Odoardi, S.; Bermejo, A. M.; Bermejo-Barrera, P.; Romolo, F. S.; Moreda-Piñeiro, A.; Strano-Rossi, S. Development of a Micro-Solid-Phase Extraction Molecularly Imprinted Polymer Technique for Synthetic Cannabinoids Assessment in Urine Followed by Liquid Chromatography–Tandem Mass Spectrometry. *J. Chromatogr. A* **2018**, *1550*, 8–20. https://doi.org/10.1016/j.chroma.2018.03.049.

(33) Kurczewska, J.; Cegłowski, M.; Pecyna, P.; Ratajczak, M.; Gajęcka, M.; Schroeder, G. Molecularly Imprinted Polymer as Drug Delivery Carrier in Alginate Dressing. *Mater. Lett.* **2017**, *201*, 46–49. https://doi.org/10.1016/j.matlet.2017.05.008.

(34) Luliński, P. Molecularly Imprinted Polymers Based Drug Delivery Devices: A Way to Application in Modern Pharmacotherapy. A Review. *Mater. Sci. Eng. C* **2017**, *76*, 1344–1353. https://doi.org/10.1016/j.msec.2017.02.138.

(35) Bodoki, A. E.; Iacob, B. C.; Bodoki, E. Perspectives of Molecularly Imprinted Polymer-Based Drug Delivery Systems in Cancer Therapy. *Polymers.* **2019**, *11* (12), 1–33. https://doi.org/10.3390/polym11122085.

(36) Haupt, K.; Medina Rangel, P. X.; Tse Sum Bui, B. Molecularly Imprinted Polymers: Antibody Mimics for Bioimaging and Therapy. *Chem. Rev.* **2020**, *120* (17), 9554–9582. https://doi.org/10.1021/acs.chemrev.0c00428.

(37) Medina Rangel, P. X.; Laclef, S.; Xu, J.; Panagiotopoulou, M.; Kovensky, J.; Tse Sum Bui, B.; Haupt, K. Solid-Phase Synthesis of Molecularly Imprinted Polymer Nanolabels: Affinity Tools for Cellular Bioimaging of Glycans. *Sci. Rep.* **2019**, *9*, 1–9. https://doi.org/10.1038/s41598-019-40348-5.

(38) Wang, H. Y.; Cao, P. P.; He, Z. Y.; He, X. W.; Li, W. Y.; Li, Y. H.; Zhang, Y. K. Targeted Imaging and Targeted Therapy of Breast Cancer Cells: Via Fluorescent Double Template-Imprinted Polymer Coated Silicon Nanoparticles by an Epitope Approach. *Nanoscale* **2019**, *11* (36), 17018–17030. https://doi.org/10.1039/c9nr04655k.

(39) Panagiotopoulou, M.; Kunath, S.; Medina-Rangel, P. X.; Haupt, K.; Tse Sum Bui, B. Fluorescent Molecularly Imprinted Polymers as Plastic Antibodies for Selective Labeling and Imaging of Hyaluronan and Sialic Acid on Fixed and Living Cells. *Biosens. Bioelectron.* **2017**, *88*, 85–93. https://doi.org/10.1016/j.bios.2016.07.080.

(40) Nestora, S.; Merlier, F.; Beyazit, S.; Prost, E.; Duma, L.; Baril, B.; Greaves, A.; Haupt, K.; Tse Sum Bui, B. Plastic Antibodies for Cosmetics : Molecularly Imprinted Polymers Scavenge Precursors of Malodors. *Angew. Chemie Int. Ed.* **2016**, *55*, 6252–6256. https://doi.org/10.1002/anie.201602076.

(41) Wang, R.; Pan, J.; Qin, M.; Guo, T. Molecularly Imprinted Nanocapsule Mimicking Phosphotriesterase for the Catalytic Hydrolysis of Organophosphorus Pesticides. *Eur. Polym. J.* **2019**, *110*, 1–8. https://doi.org/10.1016/j.eurpolymj.2018.10.045.

(42) Mohamed, S.; Balieu, S.; Petit, E.; Galas, L.; Schapman, D.; Hardouin, J.; Baati, R.; Estour, F. A Versatile and Recyclable Molecularly Imprinted Polymer as an Oxidative Catalyst of Sulfur Derivatives: A New Possible Method for Mustard Gas and v Nerve Agent Decontamination. *Chem. Commun.* **2019**, *55* (88), 13243–13246. https://doi.org/10.1039/c9cc04928b.

(43) Mathew, D.; Thomas, B.; Devaky, K. S. Design, Synthesis and Characterization of

Enzyme-Analogue-Built Polymer Catalysts as Artificial Hydrolases. *Artif. Cells, Nanomedicine Biotechnol.* **2019**, *47* (1), 1149–1172. https://doi.org/10.1080/21691401.2019.1576703.

(44) Rico-Yuste, A.; Carrasco, S. Molecularly Imprinted Polymer-Based Hybrid Materials for the Development of Optical Sensors. *Polymers.* **2019**, *11* (7), 1173. https://doi.org/10.3390/polym11071173.

(45) Saylan, Y.; Akgönüllü, S.; Yavuz, H.; Ünal, S.; Denizli, A. Molecularly Imprinted Polymer Based Sensors for Medical Applications. *Sensors* **2019**, *19* (6), 1–19. https://doi.org/10.3390/s19061279.

(46) Uzun, L.; Turner, A. P. F. Molecularly-Imprinted Polymer Sensors: Realising Their Potential. *Biosens. Bioelectron.* **2016**, *76*, 131–144. https://doi.org/10.1016/j.bios.2015.07.013.

(47) Chiappini, A.; Pasquardini, L.; Bossi, A. M. Molecular Imprinted Polymers Coupled to Photonic Structures in Biosensors: The State of Art. *Sensors* **2020**, *20* (18), 5069. https://doi.org/10.3390/s20185069.

(48) Sharma, P. S.; Pietrzyk-Le, A.; D'Souza, F.; Kutner, W. Electrochemically Synthesized Polymers in Molecular Imprinting for Chemical Sensing. *Anal. Bioanal. Chem.* **2012**, *402*, 3177–3204. https://doi.org/10.1007/s00216-011-5696-6.

(49) Ambrosini, S.; Beyazit, S.; Haupt, K.; Tse Sum Bui, B. Solid-Phase Synthesis of Molecularly Imprinted Nanoparticles for Protein Recognition. *Chem. Commun.* **2013**, *49*

(60), 6746–6748. https://doi.org/10.1039/c3cc41701h.

(50) Hoshino, Y.; Kodama, T.; Okahata, Y.; Shea, K. J. Peptide Imprinted Polymer Nanoparticles: A Plastic Antibody. *J. Am. Chem. Soc.* **2008**, *130* (46), 15242–15243. https://doi.org/10.1021/ja8062875.

(51) Székely, A.; Klussmann, M. Molecular Radical Chain Initiators for Ambient- to Low-Temperature Applications. *Chem. Asian J.* **2019**, *14* (1), 105–115. https://doi.org/10.1002/asia.201801636.

(52) Ehlers, F.; Barth, J.; Vana, P. Kinetics and Thermodynamics of Radical Polymerization. In *Fundamentals of Controlled/Living Radical Polymerization*; Tsarevsky, N., Sumerlin, B., Eds.; The Royal Society of Chemistry, 2013; pp 1–59. https://doi.org/10.1039/9781849737425-00001.

(53) O'Shannessy, D. J.; Ekberg, B.; Mosbach, K. Molecular Imprinting of Amino Acid Derivatives at Low Temperature (0°C) Using Photolytic Homolysis of Azobisnitriles. *Anal. Biochem.* **1989**, *177* (1), 144–149. https://doi.org/10.1016/0003-2697(89)90029-8.

(54) Söylemez, M. A.; Güven, O. Preparation and Detailed Structural Characterization of Penicillin G Imprinted Polymers by PALS and XPS. *Radiat. Phys. Chem.* **2019**, *159*, 174–180. https://doi.org/10.1016/j.radphyschem.2019.02.050.

(55) Lu, Y.; Li, C.; Wang, X.; Sun, P.; Xing, X. Influence of Polymerization Temperature on the Molecular Recognition of Imprinted Polymers. *J. Chromatogr. B Anal. Technol. Biomed. Life Sci.* **2004**, *804* (1), 53–59. https://doi.org/10.1016/j.jchromb.2003.10.013.

(56) Piletsky, S. A.; Piletska, E. V.; Karim, K.; Freebairn, K. W.; Legge, C. H.; Turner, A. P. F. Polymer Cookery: Influence of Polymerization Conditions on the Performance of Molecularly Imprinted Polymers. *Macromolecules* **2002**, *35* (19), 7499–7504. https://doi.org/10.1021/ma0205562.

(57) Quinn, J. F.; Davis, T. P.; Barner, L.; Barner-Kowollik, C. The Application of Ionizing Radiation in Reversible Addition-Fragmentation Chain Transfer (RAFT) Polymerization: Renaissance of a Key Synthetic and Kinetic Tool. *Polymer.* **2007**, *48* (22), 6467–6480. https://doi.org/10.1016/j.polymer.2007.08.043.

(58) Chen, M.; Zhong, M.; Johnson, J. A. Light-Controlled Radical Polymerization: Mechanisms, Methods, and Applications. *Chem. Rev.* **2016**, *116* (17), 10167–10211. https://doi.org/10.1021/acs.chemrev.5b00671.

(59) Zhang, H. Recent Advances in Macromolecularly Imprinted Polymers by Controlled Radical Polymerization Techniques. *Mol. Imprinting* **2015**, *3* (1), 35–46. https://doi.org/10.1515/molim-2015-0005.

(60) Zhang, H. Controlled/"living" Radical Precipitation Polymerization: A Versatile Polymerization Technique for Advanced Functional Polymers. *Eur. Polym. J.* **2013**, *49* (3), 579–600. https://doi.org/10.1016/j.eurpolymj.2012.12.016.

(61) Salian, V. D.; Vaughan, A. D.; Byrne, M. E. The Role of Living/Controlled Radical Polymerization in the Formation of Improved Imprinted Polymers. *J. Mol. Recognit.* **2012**, *25* (6), 361–369. https://doi.org/10.1002/jmr.2168.

(62) Corrigan, N.; Yeow, J.; Judzewitsch, P.; Xu, J.; Boyer, C. Seeing the Light: Advancing Materials Chemistry through Photopolymerization. *Angew. Chemie Int. Ed.* **2019**, *58* (16), 5170–5189. https://doi.org/10.1002/anie.201805473.

(63) Dietlin, C.; Schweizer, S.; Xiao, P.; Zhang, J.; Morlet-Savary, F.; Graff, B.; Fouassier, J. P.; Lalevée, J. Photopolymerization upon LEDs: New Photoinitiating Systems and Strategies. *Polym. Chem.* **2015**, *6* (21), 3895–3912. https://doi.org/10.1039/c5py00258c.

(64) Frick, E.; Schweigert, C.; Noble, B. B.; Ernst, H. A.; Lauer, A.; Liang, Y.; Voll, D.; Coote, M. L.; Unterreiner, A. N.; Barner-Kowollik, C. Toward a Quantitative Description of Radical Photoinitiator Structure-Reactivity Correlations. *Macromolecules* **2016**, *49* (1), 80–89. https://doi.org/10.1021/acs.macromol.5b02336.

(65) Michaudel, Q.; Kottisch, V.; Fors, B. P. Cationic Polymerization: From Photoinitiation to Photocontrol. *Angew. Chemie Int. Ed.* **2017**, *56* (33), 9670–9679. https://doi.org/10.1002/anie.201701425.

(66) Salian, V. D.; White, C. J.; Byrne, M. E. Molecularly Imprinted Polymers via Living Radical Polymerization: Relating Increased Structural Homogeneity to Improved Template Binding Parameters. *React. Funct. Polym.* **2014**, *78*, 38–46. https://doi.org/10.1016/j.reactfunctpolym.2014.02.003.

(67) Bompart, M.; Haupt, K. Molecularly Imprinted Polymers and Controlled/Living Radical Polymerization. *Aust. J. Chem.* **2009**, *62* (8), 751–761. https://doi.org/10.1071/CH09124.

(68) Karaca, N.; Temel, G.; Karaca Balta, D.; Aydin, M.; Arsu, N. Preparation of Hydrogels by

Photopolymerization of Acrylates in the Presence of Type I and One-Component Type II Photoinitiators. *J. Photochem. Photobiol. A Chem.* **2010**, *209* (1), 1–6. https://doi.org/10.1016/j.jphotochem.2009.09.017.

(69) Barner-Kowollik, C.; Vana, P.; Davis, T. P. The Kinetics of Free-Radical Polymerization. In *Handbook of Radical Polymerization*; Matyjaszewski, K., Davis, T. P., Eds.; John Wiley & Sons, Inc.: Hoboken, 2002; pp 187–261. https://doi.org/10.1002/0471220450.ch4.

(70) Beyazit, S.; Ambrosini, S.; Marchyk, N.; Palo, E.; Kale, V.; Soukka, T.; Tse Sum Bui, B.; Haupt, K. Versatile Synthetic Strategy for Coating Upconverting Nanoparticles with Polymer Shells through Localized Photopolymerization by Using the Particles as Internal Light Sources. *Angew. Chemie Int. Ed.* **2014**, *53* (34), 8919–8923. https://doi.org/10.1002/anie.201403576.

(71) Bagheri, A.; Jin, J. Photopolymerization in 3D Printing. *ACS Appl. Polym. Mater.* **2019**, *1* (4), 593–611. https://doi.org/10.1021/acsapm.8b00165.

(72) Esen, D. S.; Temel, G.; Balta, D. K.; Allonas, X.; Arsu, N. One-Component Thioxanthone Acetic Acid Derivative Photoinitiator for Free Radical Polymerization. *Photochem. Photobiol.* **2014**, *90* (2), 463–469. https://doi.org/10.1111/php.12218.

(73) Shao, J.; Huang, Y.; Fan, Q. Polymer Chemistry Photopolymerization : Status , Development And. *Polym. Chem.* **2014**, *5*, 4195–4210. https://doi.org/10.1039/c4py00072b.

(74) Tar, H.; Sevinc Esen, D.; Aydin, M.; Ley, C.; Arsu, N.; Allonas, X. Panchromatic Type II Photoinitiator for Free Radical Polymerization Based on Thioxanthone Derivative. *Macromolecules* **2013**, *46* (9), 3266–3272. https://doi.org/10.1021/ma302641d.

(75) Allushi, A.; Kutahya, C.; Aydogan, C.; Kreutzer, J.; Yilmaz, G.; Yagci, Y. Conventional Type II Photoinitiators as Activators for Photoinduced Metal-Free Atom Transfer Radical Polymerization. *Polym. Chem.* **2017**, *8* (12), 1972–1977. https://doi.org/10.1039/c7py00114b.

(76) Mokbel, H.; Graff, B.; Dumur, F.; Lalevée, J. NIR Sensitizer Operating under Long Wavelength (1064 Nm) for Free Radical Photopolymerization Processes. *Macromol. Rapid Commun.* **2020**, *41* (15), 1–5. https://doi.org/10.1002/marc.202000289.

(77) Odian, G. *Principles of Polymerization*, 4th ed.; John Wiley & Sons, Inc.: Hoboken, New Jersey, 2004.

(78) Perrier, S. 50th Anniversary Perspective: RAFT Polymerization - A User Guide. *Macromolecules* **2017**, *50* (19), 7433–7447. https://doi.org/10.1021/acs.macromol.7b00767.

(79) Corrigan, N.; Jung, K.; Moad, G.; Hawker, C. J.; Matyjaszewski, K.; Boyer, C. Reversible-Deactivation Radical Polymerization (Controlled/Living Radical Polymerization): From Discovery to Materials Design and Applications. *Prog. Polym. Sci.* **2020**, *111*, 101311. https://doi.org/10.1016/j.progpolymsci.2020.101311.

(80) Sasaki, S.; Ooya, T.; Takeuchi, T. Highly Selective Bisphenol A - Imprinted Polymers

Prepared by Atom Transfer Radical Polymerization. *Polym. Chem.* **2010**, *1* (10), 1684–1688. https://doi.org/10.1039/c0py00140f.

(81) Adali-Kaya, Z.; Tse Sum Bui, B.; Falcimaigne-Cordin, A.; Haupt, K. Molecularly Imprinted Polymer Nanomaterials and Nanocomposites: Atom-Transfer Radical Polymerization with Acidic Monomers. *Angew. Chemie Int. Ed.* **2015**, *54* (17), 5192–5195. https://doi.org/10.1002/anie.201412494.

(82) Zu, B.; Pan, G.; Guo, X.; Zhang, Y.; Zhang, H. Preparation of Molecularly Imprinted Polymer Microspheres via Atom Transfer Radical Precipitation Polymerization. *J. Polym. Sci. A Polym. Chem.* **2009**, *47* (13), 3257–3270. https://doi.org/10.1002/pola.

(83) Matyjaszewski, K. Atom Transfer Radical Polymerization (ATRP): Current Status and Future Perspectives. *Macromolecules* **2012**, *45* (10), 4015–4039. https://doi.org/10.1021/ma3001719.

(84) Ramakers, G.; Wackers, G.; Trouillet, V.; Welle, A.; Wagner, P.; Junkers, T. Laser-Grafted Molecularly Imprinted Polymers for the Detection of Histamine from Organocatalyzed Atom Transfer Radical Polymerization. *Macromolecules* **2019**, *52* (6), 2304–2313. https://doi.org/10.1021/acs.macromol.8b02339.

(85) Titirici, M. M.; Sellergren, B. Thin Molecularly Imprinted Polymer Films via Reversible Addition-Fragmentation Chain Transfer Polymerization. *Chem. Mater.* **2006**, *18* (7), 1773–1779. https://doi.org/10.1021/cm052153x.

(86) Pan, G.; Zu, B.; Guo, X.; Zhang, Y.; Li, C.; Zhang, H. Preparation of Molecularly

Imprinted Polymer Microspheres via Reversible Addition-Fragmentation Chain Transfer Precipitation Polymerization. *Polymer.* **2009**, *50* (13), 2819–2825. https://doi.org/10.1016/j.polymer.2009.04.053.

(87) Gonzato, C.; Pasetto, P.; Bedoui, F.; Mazeran, P. E.; Haupt, K. On the Effect of Using RAFT and FRP for the Bulk Synthesis of Acrylic and Methacrylic Molecularly Imprinted Polymers. *Polym. Chem.* **2014**, *5* (4), 1313–1322. https://doi.org/10.1039/c3py01246h.

(88) Vaughan, A.; Zhang, J.; Byrne, M. Enhancing Therapeutic Loading and Delaying Transport via Molecular Imprinting and Living/ Controlled Polymerization. *AIChE J.* **2010**, *56* (1), 268–279. https://doi.org/10.1002/aic.

(89) Otsu, T. Iniferter Concept and Living Radical Polymerization. *J. Polym. Sci. A Polym. Chem.* **2000**, *38* (12), 2121–2136. https://doi.org/10.1002/(SICI)1099-0518(20000615)38:12<2121::AID-POLA10>3.0.CO;2-X.

(90) Li, J.; Zu, B.; Zhang, Y.; Guo, X.; Zhang, H. One-Pot Synthesis of Surface-Functionalized Molecularly Imprinted Polymer Microspheres by Iniferter-Induced '"Living"' Radical Precipitation Polymerization. *J. Polym. Sci. A Polym. Chem.* **2010**, *48* (15), 3217–3228. https://doi.org/10.1002/pola.

(91) Pérez-Moral, N.; Mayes, A. G. Molecularly Imprinted Multi-Layer Core-Shell Nanoparticles - A Surface Grafting Approach. *Macromol. Rapid Commun.* **2007**, *28* (22), 2170–2175. https://doi.org/10.1002/marc.200700532.

(92) Çakir, P.; Cutivet, A.; Resmini, M.; Bui, B. T. S.; Haupt, K. Protein-Size Molecularly

Imprinted Polymer Nanogels as Synthetic Antibodies, by Localized Polymerization with Multi-Initiators. *Adv. Mater.* **2013**, *25* (7), 1048–1051. https://doi.org/10.1002/adma.201203400.

(93) Bonomi, P.; Attieh, M. D.; Gonzato, C.; Haupt, K. A New Versatile Water-Soluble Iniferter Platform for the Preparation of Molecularly Imprinted Nanoparticles by Photopolymerisation in Aqueous Media. *Chem. Eur. J.* **2016**, *22* (29), 10150–10154. https://doi.org/10.1002/chem.201600750.

(94) Xu, J.; Shanmugam, S.; Corrigan, N. A.; Boyer, C. Catalyst-Free Visible Light-Induced RAFT Photopolymerization. In *Controlled Radical Polymerization: Mechanisms*; Matyjaszewski, K., Sumerlin, B., Tsarevsky, N., Chiefari, J., Eds.; American Chemical Society: Washington, DC, 2015; pp 247–267. https://doi.org/10.1021/bk-2015-1187.ch013.

(95) Garcia-Soto, M. J.; Haupt, K.; Gonzato, C. Synthesis of Molecularly Imprinted Polymers by Photo-Iniferter Polymerization under Visible Light. *Polym. Chem.* **2017**, *8* (33), 4830–4834. https://doi.org/10.1039/C7PY01113J.

(96) Urraca, J. L.; Barrios, C. A.; Canalejas-Tejero, V.; Orellana, G.; Moreno-Bondi, M. C. Molecular Recognition with Nanostructures Fabricated by Photopolymerization within Metallic Subwavelength Apertures. *Nanoscale* **2014**, *6* (15), 8656–8663. https://doi.org/10.1039/c4nr01129e.

(97) Rubens, M.; Latsrisaeng, P.; Junkers, T. Visible Light-Induced Iniferter Polymerization of Methacrylates Enhanced by Continuous Flow. *Polym. Chem.* **2017**, *8* (42), 6496–6505.

https://doi.org/10.1039/c7py01157a.

(98) Benedikt, S.; Moszner, N.; Liska, R. Benzoyl Phenyltelluride as Highly Reactive Visible-Light TERP- Reagent for Controlled Radical Polymerization. *Macromolecules* **2014**, *47* (16), 5526–5531.

(99) Ding, C.; Fan, C.; Jiang, G.; Zhang, J.; Li, X.; Li, N.; Pan, X.; Zhang, Z.; Zhang, W.; Zhu, J.; Zhu, X. Diselenide Mediated Controlled Radical Polymerization under Visible Light Irradiation: Mechanism Investigation and α,ω-Ditelechelic Polymers. *Polym. Chem.* **2015**, *6* (35), 6416–6423. https://doi.org/10.1039/c5py00803d.

(100) Fors, B. P.; Hawker, C. J. Control of a Living Radical Polymerization of Methacrylates by Light. *Angew. Chemie Int. Ed.* **2012**, *51* (35), 8850–8853. https://doi.org/10.1002/anie.201203639.

(101) Lee, I. H.; Discekici, E. H.; Anastasaki, A.; De Alaniz, J. R.; Hawker, C. J. Controlled Radical Polymerization of Vinyl Ketones Using Visible Light. *Polym. Chem.* **2017**, *8* (21), 3351–3356. https://doi.org/10.1039/c7py00617a.

(102) Seo, S. E.; Discekici, E. H.; Zhang, Y.; Bates, C. M.; Hawker, C. J. Surface-Initiated PET-RAFT Polymerization under Metal-Free and Ambient Conditions Using Enzyme Degassing. *J. Polym. Sci. A Polym. Chem.* **2019**, 70–76. https://doi.org/10.1002/pola.29438.

(103) Xu, J.; Jung, K.; Atme, A.; Shanmugam, S.; Boyer, C. A Robust and Versatile Photoinduced Living Polymerization of Conjugated and Unconjugated Monomers and Its

Oxygen Tolerance. *J. Am. Chem. Soc.* **2014**, *136* (14), 5508–5519. https://doi.org/10.1021/ja501745g.

(104) Shanmugam, S.; Xu, J.; Boyer, C. Exploiting Metalloporphyrins for Selective Living Radical Polymerization Tunable over Visible Wavelengths. *J. Am. Chem. Soc.* **2015**, *137* (28), 9174–9185. https://doi.org/10.1021/jacs.5b05274.

(105) Shanmugam, S.; Xu, J.; Boyer, C. Light-Regulated Polymerization under near-Infrared/Far-Red Irradiation Catalyzed by Bacteriochlorophyll A. *Angew. Chemie Int. Ed.* **2016**, *55* (3), 1036–1040. https://doi.org/10.1002/anie.201510037.

(106) Zhang, Z.; Corrigan, N.; Bagheri, A.; Jin, J.; Boyer, C. A Versatile 3D and 4D Printing System through Photocontrolled RAFT Polymerization Research Articles. *Angew. Chemie Int. Ed.* **2019**, *58* (50), 17954–17963. https://doi.org/10.1002/anie.201912608.

(107) Shanmugam, S.; Xu, J.; Boyer, C. Photoinduced Electron Transfer-Reversible Addition-Fragmentation Chain Transfer (PET-RAFT) Polymerization of Vinyl Acetate and N-Vinylpyrrolidinone: Kinetic and Oxygen Tolerance Study. *Macromolecules* **2014**, *47* (15), 4930–4942. https://doi.org/10.1021/ma500842u.

(108) Dadashi-Silab, S.; Doran, S.; Yagci, Y. Photoinduced Electron Transfer Reactions for Macromolecular Syntheses. *Chem. Rev.* **2016**, *116* (17), 10212–10275. https://doi.org/10.1021/acs.chemrev.5b00586.

(109) Escudero, D. Revising Intramolecular Photoinduced Electron Transfer (PET) from First-Principles. *Acc. Chem. Res.* **2016**, *49* (9), 1816–1824.

https://doi.org/10.1021/acs.accounts.6b00299.

(110) Kameche, F.; Heni, W.; Telitel, S.; Ge, D.; Vidal, L.; Dumur, F.; Gigmes, D.; Lalevée, J.; Marguet, S.; Douillard, L.; Fiorini-Debuisschert, C.; Bachelot, R.; Soppera, O. Plasmon-Triggered Living Photopolymerization for Elaboration of Hybrid Polymer/Metal Nanoparticles. *Mater. Today* **2020**, *40*, 38–47. https://doi.org/10.1016/j.mattod.2020.03.023.

(111) Zhang, H.; Salo, D.; Kim, D. M.; Komarov, S.; Tai, Y.-C.; Berezin, M. Y. Penetration Depth of Photons in Biological Tissues from Hyperspectral Imaging in Shortwave Infrared in Transmission and Reflection Geometries. *J. Biomed. Opt.* **2016**, *21* (12), 126006. https://doi.org/10.1117/1.jbo.21.12.126006.

(112) Henderson, T. A.; Morries, L. D. Near-Infrared Photonic Energy Penetration: Can Infrared Phototherapy Effectively Reach the Human Brain? *Neuropsychiatr. Dis. Treat.* **2015**, *11*, 2191–2208. https://doi.org/10.2147/NDT.S78182.

(113) Cao, J.; Zhu, B.; Zheng, K.; He, S.; Meng, L.; Song, J.; Yang, H. Recent Progress in NIR-II Contrast Agent for Biological Imaging. *Front. Bioeng. Biotechnol.* **2020**, *7*, 487. https://doi.org/10.3389/fbioe.2019.00487.

(114) Strehmel, B.; Brömme, T.; Schmitz, C.; Reiner, K.; Ernst, S.; Keil, D. NIR-Dyes for Photopolymers and Laser Drying in the Graphic Industry. In *Dyes and Chomophores in Polymer Science*; Lalevée, J., Fouassier, J.-P., Eds.; John Wiley & Sons, Inc.: Hoboken, 2015; pp 213–249. https://doi.org/10.1002/9781119006671.ch7.

(115) Nagtegaele, P.; Galstian, T. V. Holographic Characterization of near Infra Red Photopolymerizable Materials. *Synth. Met.* **2002**, *127* (1–3), 85–87. https://doi.org/10.1016/S0379-6779(01)00601-4.

(116) Schmitz, C.; Halbhuber, A.; Keil, D.; Strehmel, B. NIR-Sensitized Photoinitiated Radical Polymerization and Proton Generation with Cyanines and LED Arrays. *Prog. Org. Coatings* **2016**, *100*, 32–46. https://doi.org/10.1016/j.porgcoat.2016.02.022.

(117) Bonardi, A. H.; Bonardi, F.; Morlet-Savary, F.; Dietlin, C.; Noirbent, G.; Grant, T. M.; Fouassier, J. P.; Dumur, F.; Lessard, B. H.; Gigmes, D.; Lalevée, J. Photoinduced Thermal Polymerization Reactions. *Macromolecules* **2018**, *51* (21), 8808–8820. https://doi.org/10.1021/acs.macromol.8b01741.

(118) Soppera, O.; Turck, C.; Lougnot, D. J. Fabrication of Micro-Optical Devices by Self-Guiding Photopolymerization in the near IR. *Opt. Lett.* **2009**, *34* (4), 461–463. https://doi.org/10.1364/ol.34.000461.

(119) Dika, I.; Malval, J. P.; Soppera, O.; Bardinal, V.; Barat, D.; Turck, C.; Spangenberg, A.; Bruyant, A. Near-Infrared Photopolymerization: Initiation Process Assisted by Self-Quenching and Triplet-Triplet Annihilation of Excited Cyanine Dyes. *Chem. Phys. Lett.* **2011**, *515* (1–3), 91–95. https://doi.org/10.1016/j.cplett.2011.08.091.

(120) Dika, I.; Diot, F.; Bardinal, V.; Malval, J.-P.; Ecoffet, C.; Bruyant, A.; Barat, D.; Reig, B.; Doucet, J.-B.; Camps, T.; Soppera, O. Near Infrared Photopolymer for Micro-Optics Applications. *J. Polym. Sci.* **2020**, *58* (13), 1–14. https://doi.org/10.1002/pol.20200106.

(121) Bonardi, A.; Bonardi, F.; Noirbent, G.; Dumur, F.; Gigmes, D.; Dietlin, C.; Lalevée, J. Free-radical Polymerization upon Near-infrared Light Irradiation, Merging Photochemical and Photothermal Initiating Methods. *J. Polym. Sci.* **2020**, *58* (2), 300–308. https://doi.org/10.1002/pol.20190079.

(122) Chia Gómez, L. P.; Spangenberg, A.; Ton, X. A.; Fuchs, Y.; Bokeloh, F.; Malval, J. P.; Tse Sum Bui, B.; Thuau, D.; Ayela, C.; Haupt, K.; Soppera, O. Rapid Prototyping of Chemical Microsensors Based on Molecularly Imprinted Polymers Synthesized by Two-Photon Stereolithography. *Adv. Mater.* **2016**, *28*, 5931–5937. https://doi.org/10.1002/adma.201600218.

(123) Fischer, J.; Mueller, J. B.; Kaschke, J.; Wolf, T. J. A.; Unterreiner, A.-N.; Wegener, M. Three-Dimensional Multi-Photon Direct Laser Writing with Variable Repetition Rate. *Opt. Express* **2013**, *21* (22), 26244. https://doi.org/10.1364/oe.21.026244.

(124) Torgersen, J.; Mironov, A. O. V.; Pucher, N.; Qin, X.; Li, Z.; Cicha, K.; Machacek, T.; Liska, R.; Jantsch, V.; Stampfl, J. Photo-Sensitive Hydrogels for Three- Dimensional Laser Microfabrication in the Presence of Whole Organisms. *J. Biomed. Opt.* **2012**, *17* (10), 15–18. https://doi.org/https://doi.org/10.1117/1.JBO.17.10.105008.

(125) Pandey, S.; Bodas, D. High-Quality Quantum Dots for Multiplexed Bioimaging: A Critical Review. *Adv. Colloid Interface Sci.* **2020**, *278*, 102137. https://doi.org/10.1016/j.cis.2020.102137.

(126) Sumanth Kumar, D.; Jai Kumar, B.; Mahesh, H. M. Quantum Nanostructures (QDs): An Overview. In *Synthesis of Inorganic Nanomaterials*; Bhagyaraj, S. M., Oluwafemi, O. S.,

Kalarikkal, N., Thomas, S., Eds.; Woodhead Publishing, 2018; pp 59–88. https://doi.org/10.1016/b978-0-08-101975-7.00003-8.

(127) Berry, C. C. Applications of Inorganic Nanoparticles for Biotechnology. In *Frontiers of Nanoscience*; de la Fuente, J. M., Grazu, V., Eds.; Elsevier LTD., 2012; Vol. 4, pp 159–180. https://doi.org/10.1016/B978-0-12-415769-9.00006-6.

(128) Panagiotopoulou, M.; Salinas, Y.; Beyazit, S.; Kunath, S.; Duma, L.; Prost, E.; Mayes, A. G.; Resmini, M.; Tse, B.; Bui, S.; Haupt, K. Molecularly Imprinted Polymer Coated Quantum Dots for Multiplexed Cell Targeting and Imaging. *Angew. Chemie Int. Ed.* **2016**, *55*, 8244–8248. https://doi.org/10.1002/anie.201601122.

(129) Zhu, X.; Zhang, J.; Liu, J.; Zhang, Y. Recent Progress of Rare-Earth Doped Upconversion Nanoparticles: Synthesis, Optimization, and Applications. *Adv. Sci.* **2019**, *6* (22), 1901358. https://doi.org/10.1002/advs.201901358.

(130) Wen, S.; Zhou, J.; Zheng, K.; Bednarkiewicz, A.; Liu, X.; Jin, D. Advances in Highly Doped Upconversion Nanoparticles. *Nat. Commun.* **2018**, *9*, 2415. https://doi.org/10.1038/s41467-018-04813-5.

(131) Kidakova, A.; Reut, J.; Rappich, J.; Öpik, A.; Syritski, V. Preparation of a Surface-Grafted Protein-Selective Polymer Film by Combined Use of Controlled/Living Radical Photopolymerization and Microcontact Imprinting. *React. Funct. Polym.* **2018**, *125*, 47–56. https://doi.org/10.1016/j.reactfunctpolym.2018.02.004.

(132) Tang, Y.; Liu, H.; Gao, J.; Liu, X.; Gao, X.; Lu, X.; Fang, G.; Wang, J.; Li, J.

Upconversion Particle@Fe3O4@molecularly Imprinted Polymer with Controllable Shell Thickness as High-Performance Fluorescent Probe for Sensing Quinolones. *Talanta* **2018**, *181*, 95–103. https://doi.org/10.1016/j.talanta.2018.01.006.

(133) Bakas, I.; Salmi, Z.; Jouini, M.; Geneste, F.; Mazerie, I.; Floner, D.; Carbonnier, B.; Yagci, Y.; Chehimi, M. M. Picomolar Detection of Melamine Using Molecularly Imprinted Polymer-Based Electrochemical Sensors Prepared by UV-Graft Photopolymerization. *Electroanalysis* **2015**, *27* (2), 429–439. https://doi.org/10.1002/elan.201400382.

(134) Panagiotopoulou, M.; Beyazit, S.; Nestora, S.; Haupt, K.; Tse Sum Bui, B. Initiator-Free Synthesis of Molecularly Imprinted Polymers by Polymerization of Self-Initiated Monomers. *Polymer.* **2015**, *66*, 43–51. https://doi.org/10.1016/j.polymer.2015.04.012.

(135) Shiraki, Y.; Tsuruta, K.; Morimoto, J.; Ohba, C.; Kawamura, A.; Yoshida, R.; Kawano, R.; Uragami, T.; Miyata, T. Preparation of Molecule-Responsive Microsized Hydrogels via Photopolymerization for Smart Microchannel Microvalves. *Macromol. Rapid Commun.* **2015**, *36* (6), 515–519. https://doi.org/10.1002/marc.201400676.

(136) Chen, J.; Bai, L. Y.; Liu, K. F.; Liu, R. Q.; Zhang, Y. P. Atrazine Molecular Imprinted Polymers: Comparative Analysis by Far-Infrared and Ultraviolet Induced Polymerization. *Int. J. Mol. Sci.* **2014**, *15* (1), 574–587. https://doi.org/10.3390/ijms15010574.

(137) Ton, X. A.; Tse Sum Bui, B.; Resmini, M.; Bonomi, P.; Dika, I.; Soppera, O.; Haupt, K. A Versatile Fiber-Optic Fluorescence Sensor Based on Molecularly Imprinted Microstructures Polymerized in Situ. *Angew. Chemie Int. Ed.* **2013**, *52* (32), 8317–8321.

https://doi.org/10.1002/anie.201301045.

(138) Fuchs, Y.; Soppera, O.; Mayes, A. G.; Haupt, K. Holographic Molecularly Imprinted Polymers for Label-Free Chemical Sensing. *Adv. Mater.* **2013**, *25* (4), 566–570. https://doi.org/10.1002/adma.201203204.

(139) Scherzer, T. Photopolymerization of Acrylates without Photoinitiators with Short-Wavelength UV Radiation: A Study with Real-Time Fourier Transform Infrared Spectroscopy. *J. Polym. Sci. A Polym. Chem.* **2004**, *42* (4), 894–901. https://doi.org/10.1002/pola.11039.

(140) Khlifi, A.; Gam-Derouich, S.; Jouini, M.; Chehimi, M. M. Melamine-Imprinted Polymer Grafts through Surface Photopolymerization Initiated by Aryl Layers from Diazonium Salts. *Food Control* **2013**, *31* (2), 379–386. https://doi.org/10.1016/j.foodcont.2012.10.013.

(141) Gam-Derouich, S.; Jouini, M.; Hassen-chehimi, D. Ben; Chehimi, M. M. Electrochimica Acta Aryl Diazonium Salt Surface Chemistry and Graft Photopolymerization for the Preparation of Molecularly Imprinted Polymer Biomimetic Sensor Layers. *Electrochim. Acta* **2012**, *73*, 45–52. https://doi.org/10.1016/j.electacta.2011.11.022.

(142) Scherzer, T.; Knolle, W.; Naumov, S.; Mehnert, R. Direct Initiation of the Photopolymerization of Acrylates by Short-Wavelength Excimer UV Radiation. *Nucl. Instruments Methods Phys. Res. Sect. B Beam Interact. with Mater. Atoms* **2003**, *208*, 271–276. https://doi.org/10.1016/S0168-583X(03)00620-7.

(143) Paruli, E.; Griesser, T.; Merlier, F.; Gonzato, C.; Haupt, K. Molecularly Imprinted Polymers by Thiol–Yne Chemistry: Making Imprinting Even Easier. *Polym. Chem.* **2019**, *10* (34), 4732–4739. https://doi.org/10.1039/c9py00403c.

(144) Luo, Q.; Yu, N.; Shi, C.; Wang, X.; Wu, J. Surface Plasmon Resonance Sensor for Antibiotics Detection Based on Photo-Initiated Polymerization Molecularly Imprinted Array. *Talanta* **2016**, *161*, 797–803. https://doi.org/10.1016/j.talanta.2016.09.049.

(145) Tavares, L. S.; Carvalho, T. C.; Romão, W.; Vaz, B. G.; Chaves, A. R. Paper Spray Tandem Mass Spectrometry Based on Molecularly Imprinted Polymer Substrate for Cocaine Analysis in Oral Fluid. *J. Am. Soc. Mass Spectrom.* **2018**, *29* (3), 566–572. https://doi.org/10.1007/s13361-017-1853-2.

(146) Luo, N.; Brian Hutchison, J.; Anseth, K. S.; Bowman, C. N. Synthesis of a Novel Methacrylic Monomer Iniferter and Its Application in Surface Photografting on Crosslinked Polymer Substrates. *J. Polym. Sci. A Polym. Chem.* **2002**, *40* (11), 1885–1891. https://doi.org/10.1002/pola.10272.

(147) Marchyk, N.; Maximilien, J.; Beyazit, S.; Haupt, K.; Sum Bui, B. T. One-Pot Synthesis of Iniferter-Bound Polystyrene Core Nanoparticles for the Controlled Grafting of Multilayer Shells. *Nanoscale* **2014**, *6* (5), 2872–2878. https://doi.org/10.1039/c3nr05295h.

(148) Tom, J. C.; Brilmayer, R.; Schmidt, J.; Andrieu-Brunsen, A. Optimisation of Surface-Initiated Photoiniferter-Mediated Polymerisation under Confinement, and the Formation of Block Copolymers in Mesoporous Films. *Polymers.* **2017**, *9* (10), 4–8. https://doi.org/10.3390/polym9100539.

(149) Nawaz, T.; Ahmad, M.; Yu, J.; Wang, S.; Wei, T. Biomimetic Detection of Progesterone by Novel Bifunctional Group Monomer Based Molecularly Imprinted Polymers Prepared in UV Light. *New J. Chem.* **2020**, *44* (17), 6992–7000. https://doi.org/10.1039/c9nj06387k.

(150) Wang, Y.; Jiao, S. Q.; Chen, X. L.; Wei, T. X. An Efficient Grafting Technique for Producing Molecularly Imprinted Film: Via Reversible Addition-Fragmentation Chain Transfer Polymerization. *Anal. Methods* **2017**, *9* (36), 5356–5364. https://doi.org/10.1039/c7ay01623a.

(151) Liu, Y.; Hu, X.; Liu, Z.; Meng, M.; Pan, J.; Jiang, Y.; Ni, L.; Wu, W. A Novel Dual Temperature Responsive Mesoporous Imprinted Polymer for Cd(II) Adsorption and Temperature Switchable Controlled Separation and Regeneration. *Chem. Eng. J.* **2017**, *328*, 11–24. https://doi.org/10.1016/j.cej.2017.07.034.

(152) Jing, L.; Zhang, Q.; Wang, Y.; Liu, X.; Wei, T. Surface Plasmon Resonance Sensor for Theophylline Using a Water-Compatible Molecularly Imprinted Film. *Anal. Methods* **2016**, *8* (11), 2349–2356. https://doi.org/10.1039/C6AY00028B.

(153) Demir, B.; Lemberger, M. M.; Panagiotopoulou, M.; Medina Rangel, P. X.; Timur, S.; Hirsch, T.; Tse Sum Bui, B.; Wegener, J.; Haupt, K. Tracking Hyaluronan: Molecularly Imprinted Polymer Coated Carbon Dots for Cancer Cell Targeting and Imaging. *ACS Appl. Mater. Interfaces* **2018**, *10* (4), 3305–3313. https://doi.org/10.1021/acsami.7b16225.

(154) Bossi, A. M.; Haupt, K. Tailoring a Dress to Single Protein Molecules: Proteins Can Do It Themselves through Localized Photo-Polymerization and Molecular Imprinting. *Chem.*

Eur. J. **2020**, *26* (64), 14556–14559. https://doi.org/10.1002/chem.202002787.

(155) Chen, Y.; Zhang, J.; Liu, X.; Wang, S.; Tao, J.; Huang, Y.; Wu, W.; Li, Y.; Zhou, K.; Wei, X.; Chen, S.; Li, X.; Xu, X.; Cardon, L.; Qian, Z.; Gou, M. Noninvasive in Vivo 3D Bioprinting. *Sci. Adv.* **2020**, *6* (23), eaba7406. https://doi.org/10.1126/sciadv.aba7406.

(156) Zhu, Q.; Li, X.; Xiao, Y.; Xiong, Y.; Wang, S.; Xu, C. Synthesis of Molecularly Imprinted Polymer via Visible Light Activated RAFT Polymerization in Aqueous Media at Room Temperature for Highly Selective Electrochemical Assay of Glucose. *Macromol. Chem. Phys.* **2017**, *218* (19), 1700141. https://doi.org/10.1002/macp.201700141.

(157) Cai, J.; Chen, T.; Xu, Y.; Wei, S.; Huang, W.; Liu, R.; Liu, J. A Versatile Signal-Enhanced ECL Sensing Platform Based on Molecular Imprinting Technique via PET-RAFT Cross-Linking Polymerization Using Bifunctional Ruthenium Complex as Both Catalyst and Sensing Probes. *Biosens. Bioelectron.* **2019**, *124–125*, 15–24. https://doi.org/10.1016/j.bios.2018.09.083.

(158) Rocheva, V. V.; Koroleva, A. V.; Savelyev, A. G.; Khaydukov, K. V.; Generalova, A. N.; Nechaev, A. V.; Guller, A. E.; Semchishen, V. A.; Chichkov, B. N.; Khaydukov, E. V. High-Resolution 3D Photopolymerization Assisted by Upconversion Nanoparticles for Rapid Prototyping Applications. *Sci. Rep.* **2018**, *8*, 3663. https://doi.org/10.1038/s41598-018-21793-0.

(159) Yang, J. C.; Shin, H. K.; Hong, S. W.; Park, J. Y. Lithographically Patterned Molecularly Imprinted Polymer for Gravimetric Detection of Trace Atrazine. *Sensors Actuators, B Chem.* **2015**, *216*, 476–481. https://doi.org/10.1016/j.snb.2015.04.079.

(160) Ertürk, G.; Mattiasson, B. Molecular Imprinting Techniques Used for the Preparation of Biosensors. *Sensors* **2017**, *17* (2), 288. https://doi.org/10.3390/s17020288.

(161) Trotta, F.; Biasizzo, M.; Caldera, F. Molecularly Imprinted Membranes. *Membranes.* **2012**, *2* (3), 440–477. https://doi.org/10.3390/membranes2030440.

(162) Fuchs, Y.; Soppera, O.; Haupt, K. Photopolymerization and Photostructuring of Molecularly Imprinted Polymers for Sensor Applications-A Review. *Anal. Chim. Acta* **2012**, *717*, 7–20. https://doi.org/10.1016/j.aca.2011.12.026.

(163) Hulanicki, A.; Glab, S.; Ingman, F. Chemical Sensors Definitions and Classification. *Pure Appl. Chem.* **1991**, *63* (9), 1247–1250. https://doi.org/10.1351/pac199163091247.

(164) Tran, K. T. M.; Nguyen, T. D. Lithography-Based Methods to Manufacture Biomaterials at Small Scales. *J. Sci. Adv. Mater. Devices* **2017**, *2* (1), 1–14. https://doi.org/10.1016/j.jsamd.2016.12.001.

(165) Aasime, A.; Hamouda, F. Conventional and Un-Conventional Lithography for Fabricating Thin Film Functional Devices. In *Modern technologies for creating the thin-film systems and coatings*; Nikitenkov, N., Ed.; IntechOpen, 2017; pp 43–58. https://doi.org/http://dx.doi.org/10.5772/57353.

(166) Higuera, G. A.; Truckenmüller, R. K.; Zhang, R.; Pernagallo, S.; Guillemot, F.; Moroni, L. Upscaling of High–Throughput Material Platforms in Two and Three Dimensions. In *Materiomics: High-Throughput Screening of Biomaterial Properties*; de Boer, J., van Blitterswijk, C., Eds.; Cambridge University Press: Cambridge, 2013; pp 133–154.

https://doi.org/10.1017/CBO9781139061414.009.

(167) Traub, M. C.; Longsine, W.; Truskett, V. N. Advances in Nanoimprint Lithography. *Annu. Rev. Chem. Biomol. Eng.* **2016**, *7* (1), 583–604. https://doi.org/10.1146/annurev-chembioeng-080615-034635.

(168) Hasan, R. M. M.; Luo, X. Promising Lithography Techniques for Next-Generation Logic Devices. *Nanomanufacturing Metrol.* **2018**, *1*, 67–81. https://doi.org/10.1007/s41871-018-0016-9.

(169) Madou, M. J. *Manufacturing Techniques for Microfabrication and Nanotechnology*, 1st ed.; CRC Press: Boca Raton, 2011. https://doi.org/https://doi.org/10.1201/9781439895306.

(170) Lawson, R. A.; Robinson, A. P. G. Overview of Materials and Processes for Lithography. In *Frontiers of Nanoscience*; Robinson, A. P. G., Lawson, R. A., Eds.; Elsevier Ltd., 2016; Vol. 11, pp 1–90. https://doi.org/10.1016/B978-0-08-100354-1.00001-6.

(171) Papadopoulos, C. *Nanofabrication: Principles and Applications*; Springer Nature: Victoria, 2016. https://doi.org/10.4324/9780203489680-7.

(172) Sakai, K. High-Index Immersion Lithography. In *Recent Advances in Nanofabrication Techniques and Applications*; Cui, B., Ed.; IntechOpen, 2011; pp 397–416. https://doi.org/10.5772/23630.

(173) Kwak, M. K.; Guo, L. J. Phase-Shift Lithography. In *Encyclopedia of Microfluidics and Nanofluidics*; Springer Science+Business Media, 2014; pp 1–10.

https://doi.org/10.1007/978-3-642-27758-0.

(174) Sanders, D. P. Advances in Patterning Materials for 193 Nm Immersion Lithography. *Chem. Rev.* **2010**, *110* (1), 321–360. https://doi.org/10.1021/cr900244n.

(175) Martinez-Chapa, S. O.; Salazar, A.; Madou, M. J. Two-Photon Polymerization as a Component of Desktop Integrated Manufacturing Platforms. In *Three-Dimensional Microfabrication Using Two-Photon Polymerization: Fundamentals, Technology, and Applications*; Baldacchini, T., Ed.; Elsevier Inc., 2016; pp 374–416. https://doi.org/10.1016/B978-0-323-35321-2.00019-4.

(176) Fourkas, J. T. Fundamentals of Two-Photon Fabrication. In *Three-Dimensional Microfabrication Using Two-Photon Polymerization*; Baldacchini, T., Ed.; Elsevier Inc., 2016; pp 45–61. https://doi.org/10.1016/B978-0-323-35321-2/00003-0.

(177) Bertsch, A.; Renaud, P. Microstereolithography. In *Three-Dimensional Microfabrication Using Two-Photon Polymerization*; Baldacchini, T., Ed.; Elsevier Inc., 2016; pp 20–44. https://doi.org/10.1016/B978-0-323-35321-2/00002-9.

(178) Gan, Z.; Cao, Y.; Evans, R. A.; Gu, M. Three-Dimensional Deep Sub-Diffraction Optical Beam Lithography with 9 Nm Feature Size. *Nat. Commun.* **2013**, *4*, 2061. https://doi.org/10.1038/ncomms3061.

(179) Spangenberg, A.; Hobeika, N.; Stehlin, F.; Malval, J.; Wieder, F.; Prabhakaran, P.; Baldeck, P.; Soppera, O. Recent Advances in Two-Photon Stereolithography. In *Updates in advanced lithography*; Hosaka, S., Ed.; IntechOpen, 2013; pp 35–63.

https://doi.org/10.5772/56165.

(180) Haske, W.; Chen, V. W.; Hales, J. M.; Dong, W.; Barlow, S.; Marder, S. R.; Perry, J. W. 65 Nm Feature Sizes Using Visible Wavelength 3-D Multiphoton Lithography. *Opt. Express* **2007**, *15* (6), 3426. https://doi.org/10.1364/oe.15.003426.

(181) Jiang, L.; Xiong, W.; Zhou, Y.; Liu, Y.; Huang, X.; Li, D.; Baldacchini, T.; Jiang, L.; Lu, Y. Performance Comparison of Acrylic and Thiol-Acrylic Resins in Two-Photon Polymerization. *Opt. Express* **2016**, *24* (12), 13687. https://doi.org/10.1364/oe.24.013687.

(182) Liu, Y.; Wang, H.; Ho, J.; Ng, R. C.; Ng, R. J. H.; Hall-Chen, V. H.; Koay, E. H. H.; Dong, Z.; Liu, H.; Qiu, C.-W.; Greer, J. R.; Yang, J. K. W. Structural Color Three-Dimensional Printing by Shrinking Photonic Crystals. *Nat. Commun.* **2019**, *10*, 4340. https://doi.org/10.1038/s41467-019-12360-w.

(183) Fuchs, Y.; Linares, A. V.; Mayes, A. G.; Haupt, K.; Soppera, O. Ultrathin Selective Molecularly Imprinted Polymer Microdots Obtained by Evanescent Wave Photopolymerization. *Chem. Mater.* **2011**, *23* (16), 3645–3651. https://doi.org/10.1021/cm2009829.

(184) Milosevic, M. On the Nature of the Evanescent Wave. *Appl. Spectrosc.* **2013**, *67* (2), 126–131. https://doi.org/10.1366/12-06707.

(185) Taitt, C. R.; Anderson, G. P.; Ligler, F. S. Evanescent Wave Fluorescence Biosensors: Advances of the Last Decade. *Biosens. Bioelectron.* **2016**, *76*, 103–112. https://doi.org/10.1016/j.bios.2015.07.040.

(186) Zhou, X.; Soppera, O.; Plain, J.; Jradi, S.; Wei Sun, X.; Volkan Demir, H.; Yang, X.; Deeb, C.; Gray, S. K.; Wiederrecht, G. P.; Bachelot, R. Plasmon-Based Photopolymerization: Near-Field Probing, Advanced Photonic Nanostructures and Nanophotochemistry. *J. Opt.* **2014**, *16* (11), 114002. https://doi.org/10.1088/2040-8978/16/11/114002.

(187) Deeb, C.; Ecoffet, C.; Bachelot, R.; Plain, J.; Bouhelier, A.; Soppera, O. Plasmon-Based Free-Radical Photopolymerization: Effect of Diffusion on Nanolithography Processes. *J. Am. Chem. Soc.* **2011**, *133* (27), 10535–10542. https://doi.org/10.1021/ja201636y.

(188) Ibn El Ahrach, H.; Bachelot, R.; Vial, A.; Lérondel, G.; Plain, J.; Royer, P.; Soppera, O. Spectral Degeneracy Breaking of the Plasmon Resonance of Single Metal Nanoparticles by Nanoscale Near-Field Photopolymerization. *Phys. Rev. Lett.* **2007**, *98* (10), 1–4. https://doi.org/10.1103/PhysRevLett.98.107402.

(189) Ge, D.; Marguet, S.; Issa, A.; Jradi, S.; Nguyen, T. H.; Nahra, M.; Béal, J.; Deturche, R.; Chen, H.; Blaize, S.; Plain, J.; Fiorini, C.; Douillard, L.; Soppera, O.; Dinh, X. Q.; Dang, C.; Yang, X.; Xu, T.; Wei, B.; Sun, X. W.; Couteau, C.; Bachelot, R. Hybrid Plasmonic Nano-Emitters with Controlled Single Quantum Emitter Positioning on the Local Excitation Field. *Nat. Commun.* **2020**, *11*, 3414. https://doi.org/10.1038/s41467-020-17248-8.

(190) Ali, M. Y.; Hung, W. N. P. Micromachining. In *Comprehensive Materials Finishing*; Hashmi, M. S. J., Ed.; Elsevier Inc., 2017; Vol. 1, pp 322–343. https://doi.org/10.1016/B978-0-12-803581-8.09156-6.

(191) Guillon, S.; Lemaire, R.; Linares, A. V.; Haupt, K.; Ayela, C. Single Step Patterning of Molecularly Imprinted Polymers for Large Scale Fabrication of Microbiochips. *Lab Chip* **2009**, *9* (20), 2987–2991. https://doi.org/10.1039/b905608d.

(192) Boysen, R. I.; Li, S.; Chowdhury, J.; Schwarz, L. J.; Hearn, M. T. W. Selectivity Optimisation of Biomimetic Molecularly Imprinted Polymer Thin Films. *Microelectron. Eng.* **2012**, *97*, 81–84. https://doi.org/10.1016/j.mee.2012.03.026.

(193) Li, L.; Lu, Y.; Bie, Z.; Chen, H. Y.; Liu, Z. Photolithographic Boronate Affinity Molecular Imprinting: A General and Facile Approach for Glycoprotein Imprinting. *Angew. Chemie Int. Ed.* **2013**, *52* (29), 7451–7454. https://doi.org/10.1002/anie.201207950.

(194) Dezest, D.; Leïchlé, T.; Teerapanich, P.; Matthieu, F.; Tse Sum Bui, B.; Haupt, K.; Nicu, L. Multiplexed Functionalization of Nanoelectromechanical Systems with Photopatterned Molecularly Imprinted Polymers. *J. Micromechanics Microengineering* **2019**, *29* (2), 025013. https://doi.org/https://doi.org/10.1088/1361-6439/aaf84e.

(195) Linares, A. V.; Falcimaigne-Cordin, A.; Gheber, L. A.; Haupt, K. Patterning Nanostructured, Synthetic, Polymeric Receptors by Simultaneous Projection Photolithography, Nanomolding, and Molecular Imprinting. *Small* **2011**, *7* (16), 2318–2325. https://doi.org/10.1002/smll.201100248.

(196) LaFratta, C. N.; Fourkas, J. T.; Baldacchini, T.; Farrer, R. A. Multiphoton Fabrication. *Angew. Chemie Int. Ed.* **2007**, *46* (33), 6238–6258. https://doi.org/10.1002/anie.200603995.

(197) Wu, Y.; Chen, R.; Zhao, G.; Chen, X.; Qu, X.; Liu, Y. Effect of Graphite Particles as Additive on the Curing Behaviour of β-Tricalcium Phosphate Suspensions and Scaffold Fabrication by Digital Light Processing. *J. Eur. Ceram. Soc.* **2020**, *40* (12), 4323–4331. https://doi.org/10.1016/j.jeurceramsoc.2020.05.013.

(198) Sun, C.; Zhang, X. Experimental and Numerical Investigations on Microstereolithography of Ceramics. *J. Appl. Phys.* **2002**, *92* (8), 4796–4802. https://doi.org/10.1063/1.1503410.

(199) Conrad, P. G.; Nishimura, P. T.; Aherne, D.; Schwartz, B. J.; Wu, D.; Fang, N.; Zhang, X.; Roberts, M. J.; Shea, K. J. Functional Molecularly Imprinted Polymer Microstructures Fabricated Using Microstereolithography. *Adv. Mater.* **2003**, *15* (18), 1541–1544. https://doi.org/10.1002/adma.200304602.

(200) Crowe, J. A.; El-Tamer, A.; Nagel, D.; Koroleva, A. V.; Madrid-Wolff, J.; Olarte, O. E.; Sokolovsky, S.; Estevez-Priego, E.; Ludl, A.-A.; Soriano, J.; Loza-Alvarez, P.; Chichkov, B. N.; Hill, E. J.; Parri, H. R.; Rafailov, E. U. Development of Two-Photon Polymerised Scaffolds for Optical Interrogation and Neurite Guidance of Human IPSC-Derived Cortical Neuronal Networks. *Lab Chip* **2020**, *20*, 1792–1806. https://doi.org/10.1039/c9lc01209e.

(201) Trautmann, A.; Rüth, M.; Lemke, H. D.; Walther, T.; Hellmann, R. Two-Photon Polymerization Based Large Scaffolds for Adhesion and Proliferation Studies of Human Primary Fibroblasts. *Opt. Laser Technol.* **2018**, *106*, 474–480. https://doi.org/10.1016/j.optlastec.2018.05.008.

(202) Lee, M. R.; Phang, I. Y.; Cui, Y.; Lee, Y. H.; Ling, X. Y. Shape-Shifting 3D Protein

Microstructures with Programmable Directionality via Quantitative Nanoscale Stiffness Modulation. *Small* **2015**, *11* (6), 740–748. https://doi.org/10.1002/smll.201401343.

(203) Parkatzidis, K.; Chatzinikolaidou, M.; Koufakis, E.; Kaliva, M.; Farsari, M.; Vamvakaki, M. Multi-Photon Polymerization of Bio-Inspired, Thymol-Functionalized Hybrid Materials with Biocompatible and Antimicrobial Activity. *Polym. Chem.* **2020**, *11*, 4078–4083. https://doi.org/10.1039/d0py00281j.

(204) Saha, S. K.; Oakdale, J. S.; Cuadra, J. A.; Divin, C.; Ye, J.; Forien, J. B.; Bayu Aji, L. B.; Biener, J.; Smith, W. L. Radiopaque Resists for Two-Photon Lithography to Enable Submicron 3D Imaging of Polymer Parts via X-Ray Computed Tomography. *ACS Appl. Mater. Interfaces* **2018**, *10* (1), 1164–1172. https://doi.org/10.1021/acsami.7b12654.

(205) Thiele, S.; Pruss, C.; Herkommer, A. M.; Giessen, H. 3D Printed Stacked Diffractive Microlenses. *Opt. Express* **2019**, *27* (24), 35621. https://doi.org/10.1364/oe.27.035621.

(206) Wang, H.; Liu, Y.; Ruan, Q.; Liu, H.; Ng, R. J. H.; Tan, Y. S.; Wang, H.; Li, Y.; Qiu, C. W.; Yang, J. K. W. Off-Axis Holography with Uniform Illumination via 3D Printed Diffractive Optical Elements. *Adv. Opt. Mater.* **2019**, *7* (12), 1–9. https://doi.org/10.1002/adom.201900068.

(207) Ovsianikov, A.; Chichkov, B. Two-Photon Polymerization - High Resolution 3D Laser Technology and Its Applications. In *Nanoelectronics and Photonics: From Atoms to Materials, Devices and Architectures*; Korkin, A., Rosei, F., Eds.; Springer Science+Business Media, LLC: New York, 2008; pp 430–433.

(208) Lewis, A.; Taha, H.; Strinkovski, A.; Manevitch, A.; Khatchatouriants, A.; Dekhter, R.; Ammann, E. Near-Field Optics: From Subwavelength Illumination to Nanometric Shadowing. *Nat. Biotechnol.* **2003**, *21* (11), 1378–1386. https://doi.org/10.1038/nbt898.

(209) Greffet, J. J.; Carminati, R. Image Formation in Near-Field Optics. *Prog. Surf. Sci.* **1997**, *56* (3), 133–237. https://doi.org/10.1016/S0079-6816(98)00004-5.